

**NGU Report 2003.081**

**Gravity and magnetic interpretation of the  
regional deep structure of the Vøring Basin**

Report no.: 2003.081		ISSN 0800-3416	Grading: <del>Confidential until 2005</del> - Åpen
Title: Gravity and magnetic interpretation of the regional deep structure of the Vøring Basin			
Authors: Jörg Ebbing		Client: BP Norway	
County: Mid-Norwegian Continental Shelf		Commune:	
Map-sheet name (M=1:250.000)		Map-sheet no. and -name (M=1:50.000)	
Deposit name and grid-reference:		Number of pages: 41 Map enclosures: 4	Price (NOK): Kr. 480,-
Fieldwork carried out:	Date of report: 31.01.2004	Project no.: 304000	Person responsible: <i>Elisabeth A. Eide</i>
<p>Summary:</p> <p>The crustal structure in the outer Vøring Basin is investigated by forward modelling of gravity data and interpretation of the magnetic field and the isostatic state. In addition all available magnetic and gravity data for the Vøring Basin have been reprocessed.</p> <p>BP delivered depth-converted interpretation along six seismic profiles. These, together with the available results of OBS arrays, constrain the geometry of the structural models. The modelling has been done in 2D and where needed in 3D. Especially in the central and northern Vøring Basin, lateral changes in the density structures perpendicular to the seismic profiles had to be regarded to adjust the models.</p> <p>The 2D and 3D models show that the gravity field is mainly influenced by the thickness of the sediments, the depth of the Moho and the occurrence of magmatic underplating. The high density magmatic underplated material is probably related to the intrusion of sills from the Vøring Escarpment into the Vøring Basin and stops westwards of the Fles Fault Complex. To the east of the Fles Fault Complex normal lower crustal material is present instead.</p> <p>Seismic results show in the whole area deep crustal reflectors, which have been previously interpreted to be connected to magmatic underplating or top basement. The modelling results indicate that these reflections are connected to magmatic underplated structures and intracrustal reflectors. The modelling results are subsequently used to produce new maps of the depth to Basement and Moho.</p> <p>The shape of the magnetic field in the outer Vøring area suggests, in contrast to the gravity field, shallow sources, which are probably connected to igneous rocks. But in general the magnetic signature in the outer Vøring Basin shows no prominent anomalies. The main magnetic anomalies are caused by the transition to oceanic domains.</p>			
Keywords: Gravimetri	Magnetometri	Geofysikk	
Kontinentalsokkel	Modellforsk	Tredimensjonal	
Tolkning	Densitet	Isostasi	

## CONTENTS

1	INTRODUCTION.....	4
2	MAIN STRUCTURAL ELEMENTS IN THE STUDY AREA.....	4
3	DATA SETS.....	6
	3.1 SEISMIC INFORMATION.....	6
	3.2 GRAVITY DATA.....	9
	3.3 AEROMAGNETIC DATA.....	9
	3.4 BATHYMETRIC DATA.....	15
	3.5 DENSITY INFORMATION.....	16
4	FORWARD MODELLING.....	17
	4.1 Profile GVLO.....	17
	4.2 Profile VMT.....	18
	4.3 Profile VBT94.....	19
	4.4 Profile GRS.....	20
	4.5 Profile BPN.....	21
	4.6 Basement and Moho depth.....	22
5	MAGNETIC AND ISOSTATIC INVESTIGATIONS.....	34
	5.1 Magnetic interpretation.....	34
	5.2 Isostatic implications.....	34
6	DISCUSSION AND INTERPRETATION.....	35
7	ACKNOWLEDGEMENTS.....	37
8	REFERENCES.....	37
	LIST OF FIGURES, TABLES AND MAPS.....	41

## **1 INTRODUCTION**

The study is carried out by the Geological Survey of Norway (NGU) as contract work for BP Norge. The main objective of the project is to study the deep structure of selected parts of the Vøring Basin by the analysis of potential field data. This is mainly done by forward modelling along seismic profiles, which have been interpreted and depth-converted by BP.

In addition, in this project the gravity and magnetic data of the Mid-Norwegian shelf have been reprocessed during September and October 2003. These data cover the area between 2° to 8° W and 65° to 68° N.

## **2 MAIN STRUCTURAL ELEMENTS IN THE STUDY AREA**

The Vøring Margin has been extensively studied by the use of multi-channel seismic reflection data, seismic refraction data, commercial drilling on the continental shelf and scientific drilling (e.g. Skogseid et al. 1992, Doré et al. 1999, Brekke 2000, Mjelde et al. 2001, Raum et al. 2002, Mjelde et al. 2003 a, b, c).

The Vøring margin is located between 64° and 68° N, off Norway, and comprises three main geological provinces: the Trøndelag Platform, the Vøring Basin and the Vøring Marginal High (Figure 1). These segments are further separated by NE-SW striking fault systems, developed since late Caledonian times. Northward, the Vøring Margin is bounded by the Bivrost Lineament, representing the transition to the Lofoten Margin, while the East Jan Mayen Fracture Zone represents the southern boundary and represents the transition to the Møre Margin.

Early Tertiary continental break-up and initial seafloor spreading between Eurasia and Greenland was characterized by massive emplacement of magmatic rocks (e.g. Eldholm and Grue 1994). On the Vøring Margin these rocks were partially extruded on the surface as flood basalts and partially intruded as sills into the sedimentary rocks in the Vøring Basin and presumably into continental crust (Mjelde et al. 2001). This magmatic material is likely to have been emplaced as thick magmatic intrusions into the lower crust (underplating) on both sides of the Vøring Escarpment (Skogseid et al., 1992).

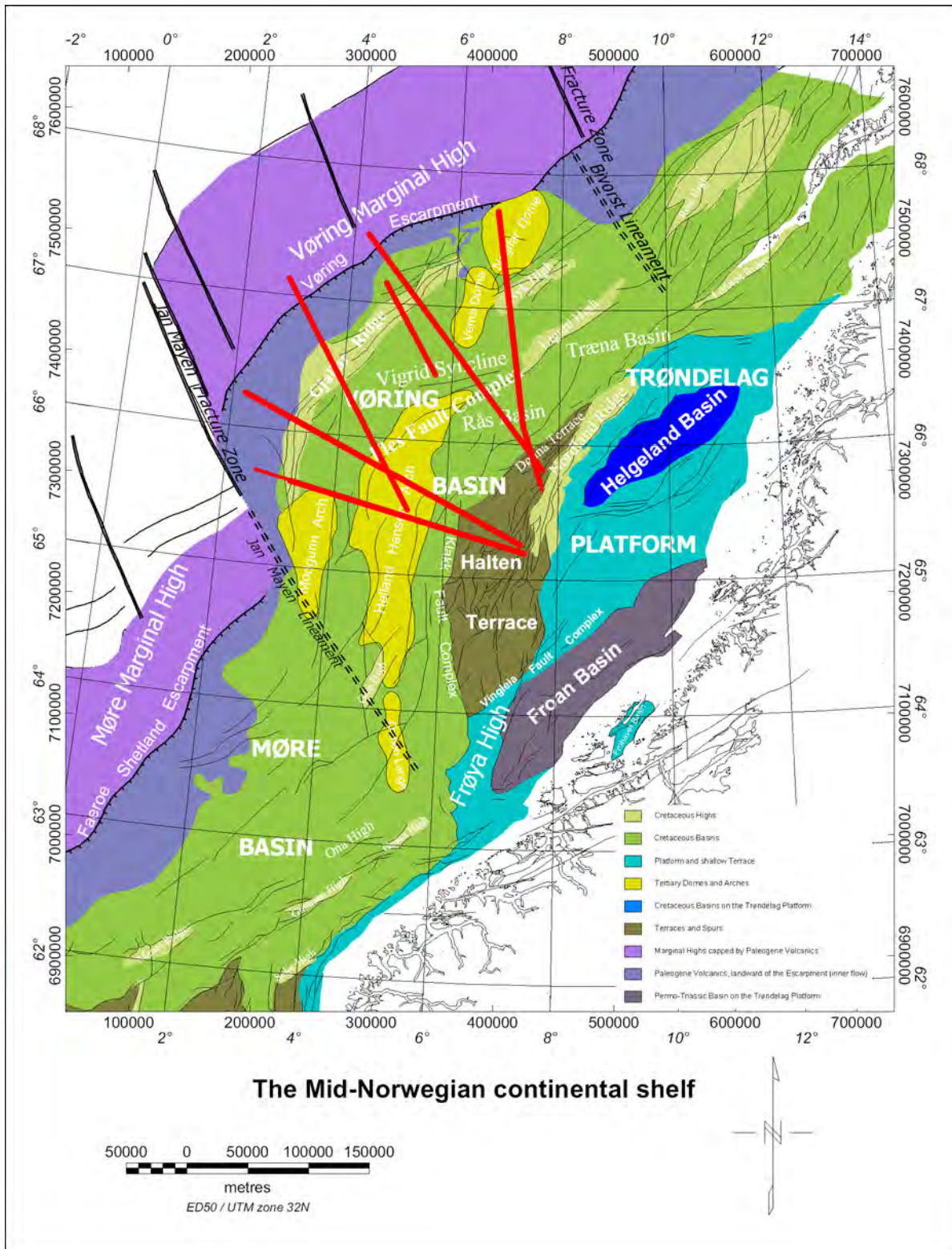


**Figure 1** Structural elements of the Mid-Norwegian Shelf and location of seismic profiles (Aarnæs 2003, after Blystad et al. 1995, Brekke 2000). The red lines indicate the position of the BP profiles.

### 3 DATA SETS

#### 3.1 Seismic information

Depth-converted interpretations along six seismic profiles were delivered by BP (see Figure 1 and 2 for location of the profiles). Table 1 shows the name as referred to in the text, the full name and the length of the interpreted profiles.

Name	Full name	Interpreted length
GVLO	GVLO99-r03-101	c. 250 km
VMT	VMT95-008A	c. 240 km
VBT94	VBT94001/001 - consists of two segments	c. 250 km
GVF	GVF2000-213	c. 85 km
GRS	GRS99-232, GRS98-120, VB-2-87r01- composite profile	c. 230 km
BPN	BPN9902 R99 02	c. 220 km

**Table 1** Overview of the interpreted profiles by BP used in this study.

The profile **GVLO** is located in the south of the study area and extends from the landward side of the Vøring Escarpment through the Vøring Basin. Within the Vøring Basin the profile crosses the Gjallar Ridge, the Vigrid Syncline, the Slettringen Ridge, the Helland Hansen Arch, the southern part of the Rås Basin and ends in the Haltern Terrace. Continuing to the southeast, the Nordland Ridge is the next main geological structure. The profile also intersects the Ocean Bottom Seismograph (OBS) array presented by Raum et al. (2002).

The southernmost of the profiles is named **VMT**. It is located close to profile GVLO and also extends from the landward side of the Vøring Escarpment through the Vøring Basin. The profile crosses the Gjallar Ridge, Modgunn Arch, Fles Fault Complex, Helland Hansen Arch, the Klakk Fault and ends in the Haltern Terrace, almost at the same location as profile GVLO. It also intersects the OBS array presented by Raum et al. (2002).

The profile **VBT94** leads from the seaward side of the Vøring Escarpment through the Fenris Graben, the Gjallar Ridge, the Vigrid Syncline, the Fles Fault Complex, the Rås Basin and ends within the Dønna Terrace. The profile crosses south of the Vema Dome and the Utgard High. The area is also covered by a several OBS arrays (Mjelde et al. 1997, Mjelde et al. 2001), which provide information on the 3D structure.

Profile **GVF** is located close to profile VBT94 and covers only the outer northern part of the Vøring Basin, transecting the Fenris Graben, the Gjallar Ridge and the Vigrid Syncline.

Profile **GRS** is located between the long seismic profiles GVLO and VBT94 in the outermost part of the Vøring Basin, crossing the Vøring Escarpment to the Vøring Marginal High, and landwards into the Gjallar Ridge. The profile is located to the west of the OBS array by Raum et al. (2002) and crosses at its southern end the profiles GVLO and VMT.

The northernmost profile is **BPN**. Unlike the other profiles, BPN has a north-south orientation and leads from the landward side of the Vøring Escarpment through the Naglfar Dome in the Hel Graben, Nyk High, Någrind Syncline, the central Rås Basin and ends within the Dønna Terrace. The profile is close to the Utgard High and crosses the Fles Fault Complex/Surt Lineament. In the Hel Graben the profile intersects the OBS array by Mjelde et al. (1997) and in the Dønna Terrace it crosses the profile GVLO.

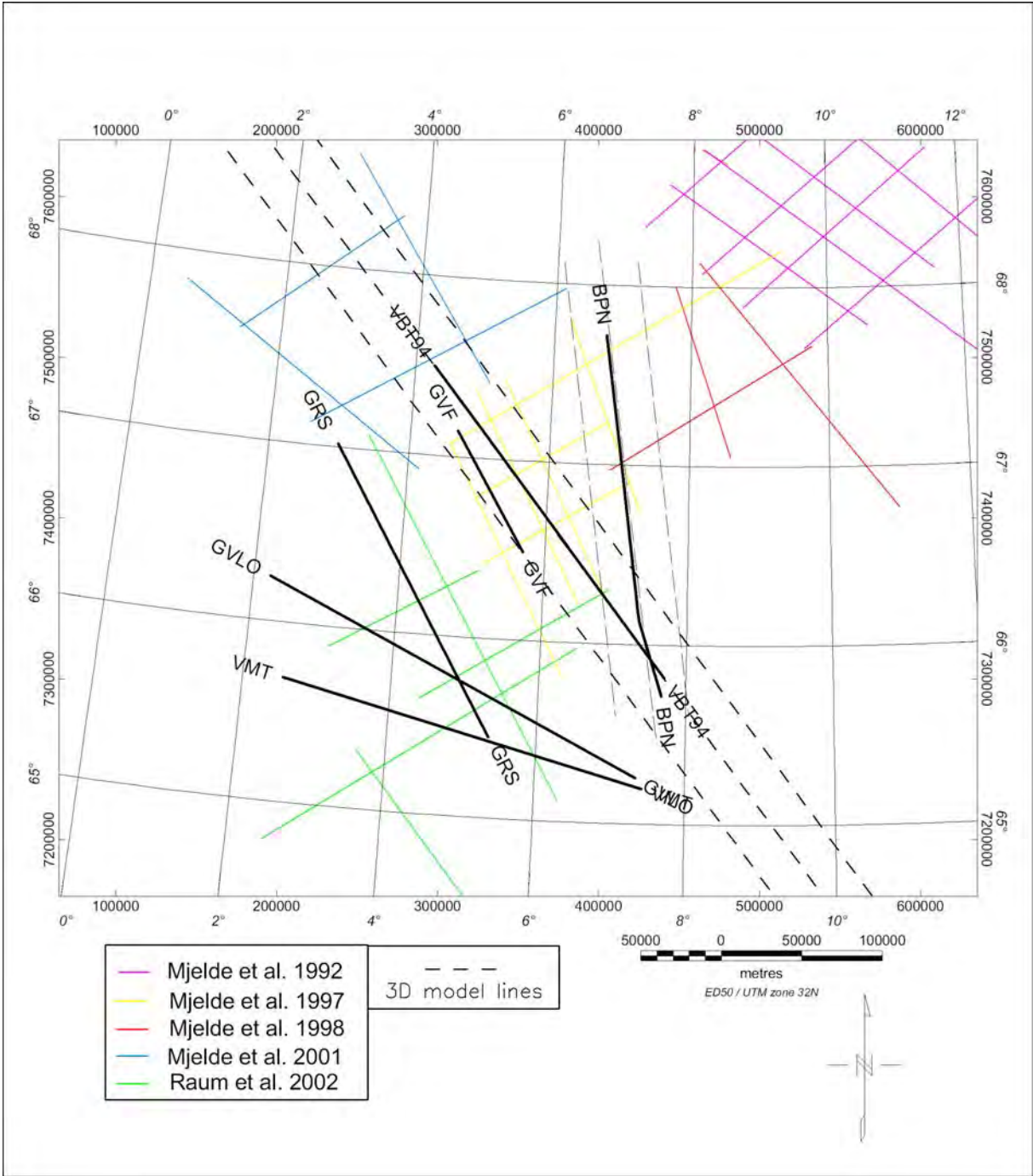


**Figure 2** Seismic profiles by BP and available OBS lines in the study area.

Interpretations of OBS arrays are available from the studies of Mjelde et al. (1992, 1997, 1998, 2001, 2003a, 2003b) and Raum et al. (2002). The results of the OBS arrays have been interpreted along profiles, providing good coverage of the study area (Fig. 2). Further, a combined study of expanded spread profiles and refraction profiles is available in Planke et al. (1991). New interpretations along long offset seismic reflection profiles are also available from Osmundsen et al. (2002). The information from these studies was considered, wherever possible, to constrain the modelling. This is especially important for regional structures (e.g. Moho boundary, crustal underplating).

Along the reflection seismic profiles depth-migrated interpretations were delivered by BP. The interpretations consist of the following horizons:

- Base Pliocene
- Mid Oligocene
- T50 - Earliest Eocene
- K90 - Base Tertiary Unconformity
- K80 - Campanian
- K72 - Coniacian
- K66 - Cenomanian
- K54 - Albian
- BCU - Base Cretaceous Unconformity

In addition some reflections within the deeper crust are marked. These reflections are interpreted to be of intracrustal origin, connected to magmatic underplating or the crust-mantle boundary. Different interpretations exist for the nature of the intracrustal reflections (e.g. Gernignon et al. 2002, 2003; Wheeler 2002). However, the information for the deeper parts of the profiles is rather crude and additional regional information from the OBS lines is needed to give a well-constrained model of the area. Identification of the origin of the deep reflections is one of the objectives of the study.

Information on the Moho depth in the study area was further considered to constrain the regional structures. New information based on the study by Kinck et al. (1993) has been published in the results of the NGU BAT-project (Basin Analysis and applied Thermochronology on the Mid Norwegian Continental Shelf, e.g. Olesen et al. 2002, Osmundsen et al. 2002).



### 3.2 Gravity data

The present study is based on measurements from approximately 59,000 km of marine gravity profiles collected by the Norwegian Petroleum Directorate, oil companies and the Norwegian Mapping Authorities, in addition to gravity data from satellite altimetry in the deep-water areas of the Norwegian Sea (Andersen & Knudsen 1998). The International Standardization Net 1971 (I.G.S.N. 71) and the Gravity Formula 1980 for normal gravity have been used to level the surveys. The compiled dataset has been interpolated to a square grid of 2 km x 2 km using the minimum curvature method. The locations of the marine profiles are shown in Figure 3, while Figure 4 shows the free-air gravity field of the Mid-Norwegian continental shelf. These gravity data are also available for BP in digital form.

Year	Area	Survey name	Operator	Length km
1980-1993	Norwegian Sea	NPD-compilation	Misc. companies	59,000
1998-99	Gjallar Ridge	GRS98/99	TGS-Nopec	3,600
1999	Gjallar Ridge south	GRSI99	TGS-Nopec	854
1996	Vøring Basin	V2VB96	Amarok-NIASA	3,630

**Table 2** Marine gravity surveys on the Mid-Norwegian continental shelf compiled for the present study (Figures 3 and 4).

### 3.3 Aeromagnetic data

A total of eight offshore aeromagnetic surveys (Fig. 5) have been compiled in the present project. Specifications for these surveys are shown in Table 3. Vintage data that were reflight in 1989, 1994 and 1998 are not included in the table, and are also excluded in the final map compilation. The pattern of flight lines generally provides data along NW-SE trending lines with a spacing of 2-5 km. The LAS-89, NAS-94, VAS-98 and RAS-03 surveys have been processed within the Ra-3 project using the loop closure method (Mauring et al. 2003). The SPT-93, VGVB-94 and aeromagnetic data on land have earlier been digitised into a 500 x 500 m matrix and the Definite Geomagnetic Reference Field (DGRF) has been subtracted (Nor. geol. unders. 1992). The area was flown at different flight altitudes and line spacing dependent on the topography. Specifications for the different sub-areas are given in Table 4. The grids were trimmed to c. 10 km overlap and merged using a minimum curvature algorithm, GRIDKNIT, developed by Geosoft (2000). The final grid shown in Figure 6 was displayed using the shaded-relief technique with illumination from the southeast.

Year	Area	Operator	Survey name	Navigation	Sensor elevation m	Line spacing km	Length km
1969	69° - 70°N	NGU	NGU-69	Decca	200	4	1,000
1973	Vøring Basin	NGU	NGU-73	Loran C	500	5	6,000
1973	Norwegian Sea	Naval Research Lab.	NRL-73		300	10	5,000
1989	Lofoten	NGU	LAS-89	GPS/ Loran C/ Syledis	250	2	24,000
1993	Hel Graben-Nyk High	World Geo-science	SPT-93	GPS	80	0.75	19,000
1994	Nordland Ridge-Helgeland Basin	NGU	NAS-94	GPS	150	2	28,000
1994	Vøring Basin	Amarok	VGVB-94 western part	GPS	140	1-3	11,000
1998	Vestfjorden	NGU	VAS-98	GPS	150	2	6,000
2000	Southern Gjallar Ridge	TGS-Nopec	VBE-AM-00	GPS	130	1-4	17,000
2003	Røst Basin	NGU	RAS-03	GPS	230	2	28,000

**Table 3** Offshore aeromagnetic surveys compiled for the present study (Figure 5 and 6).

Year	Area	Operator	Navigation	Sensor elevation	Line spacing km	Recording
1964	Andøya	NGU	Visual	150 m above ground	1	Analogue
1965	Vesterålen area	NGU	Visual	300 m above ground	2	"
1971-73	Nordland-Troms	NGU	Decca	1000 m above sea level	2	"
1971-1972	Namdalen	NGU	Visual and Decca	300 m above ground	1	"
1959-1969	Central Norway	NGU	Visual	150 m above ground	0.5	"

**Table 4** On land aeromagnetic surveys compiled for the present interpretation.

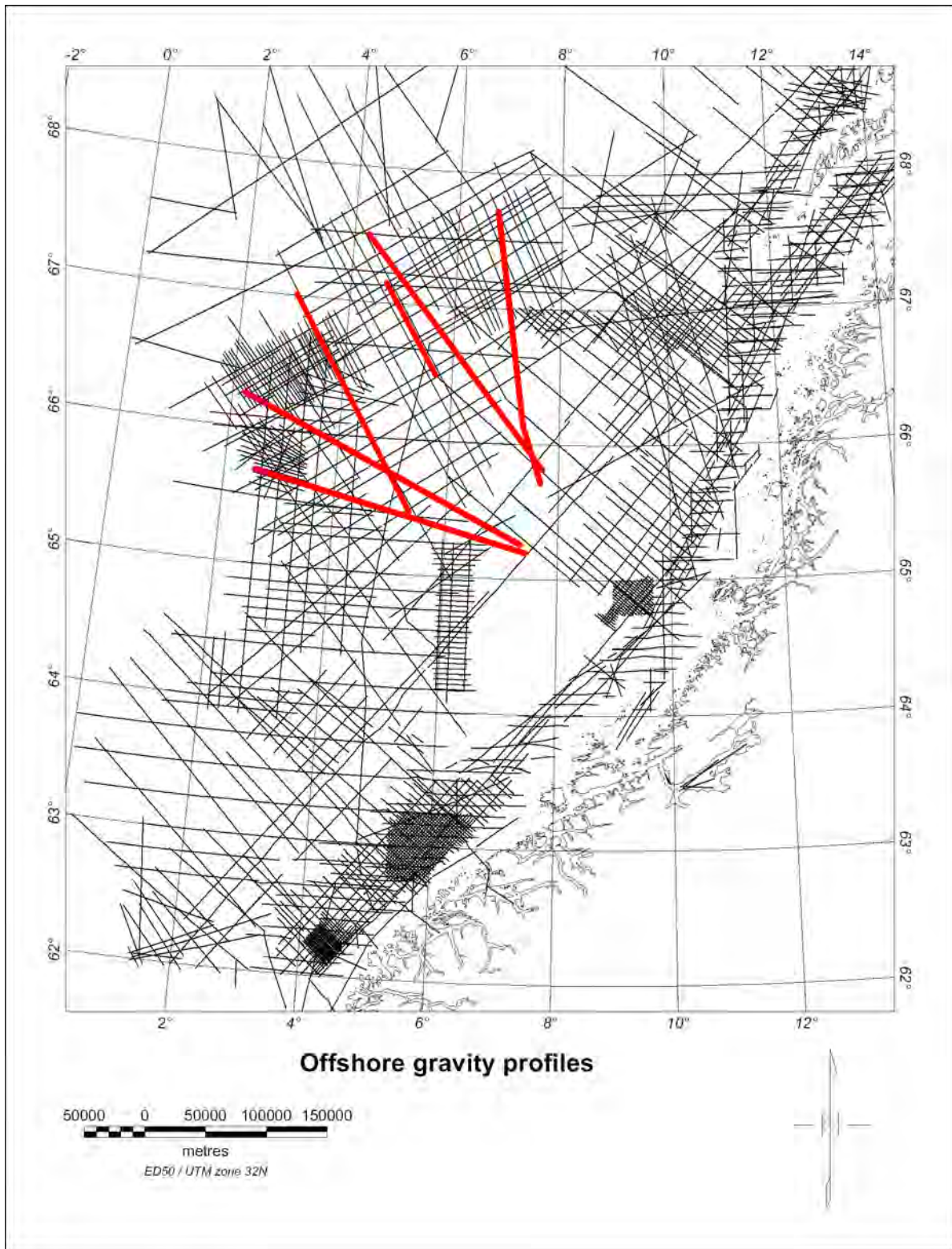


**Figure 3** Location of marine gravity profiles on the Mid-Norwegian continental shelf. Red lines indicate the studied profiles.

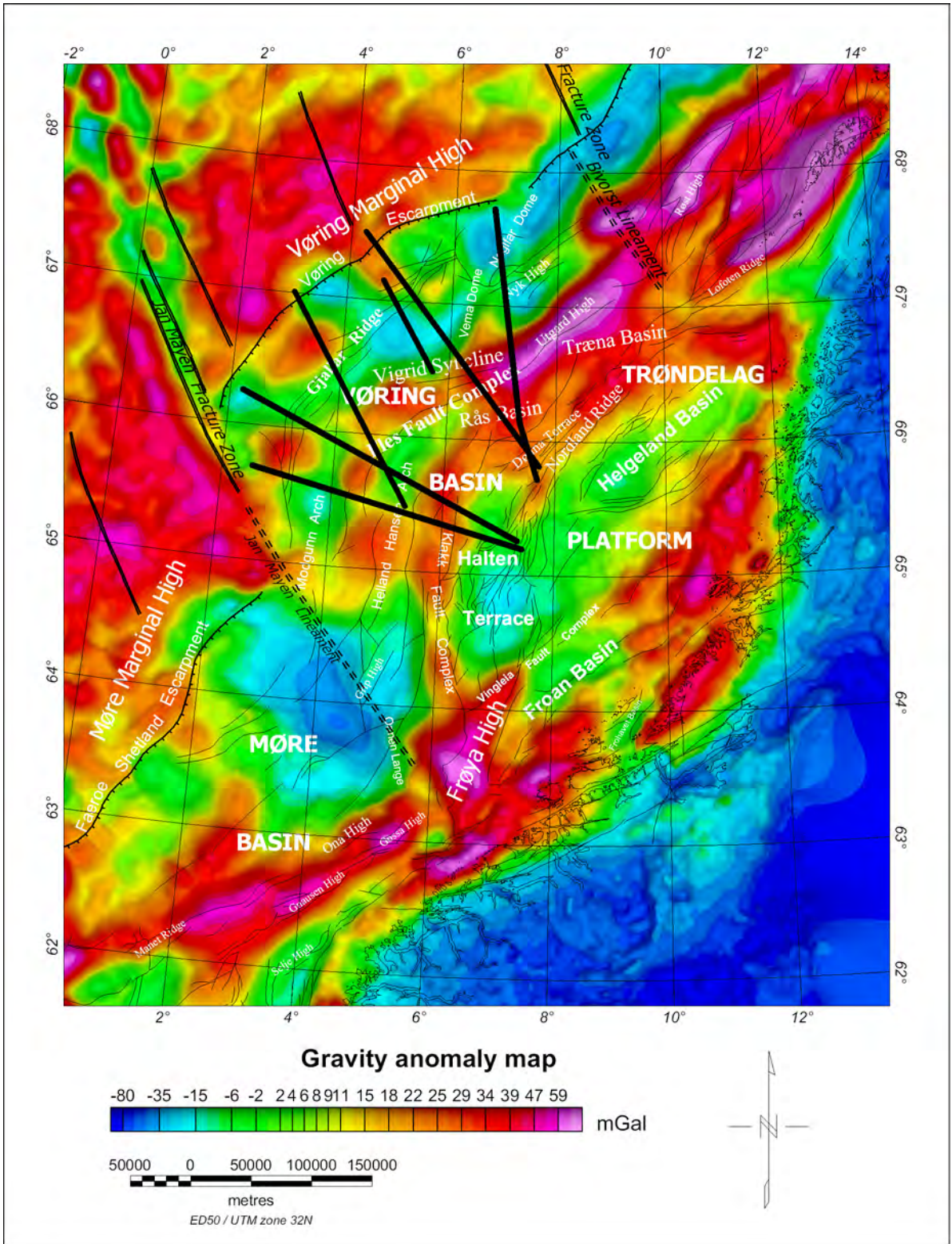


**Figure 4** The gravity anomaly of the Mid-Norwegian continental shelf is produced by a combination of marine gravity profiles and satellite data (Andersen and Knudsen 1998) in the oceanic basin. The map is showing free-air anomalies offshore and Bouguer anomalies onshore. See Fig. 3 for the location of the marine gravity profiles used.

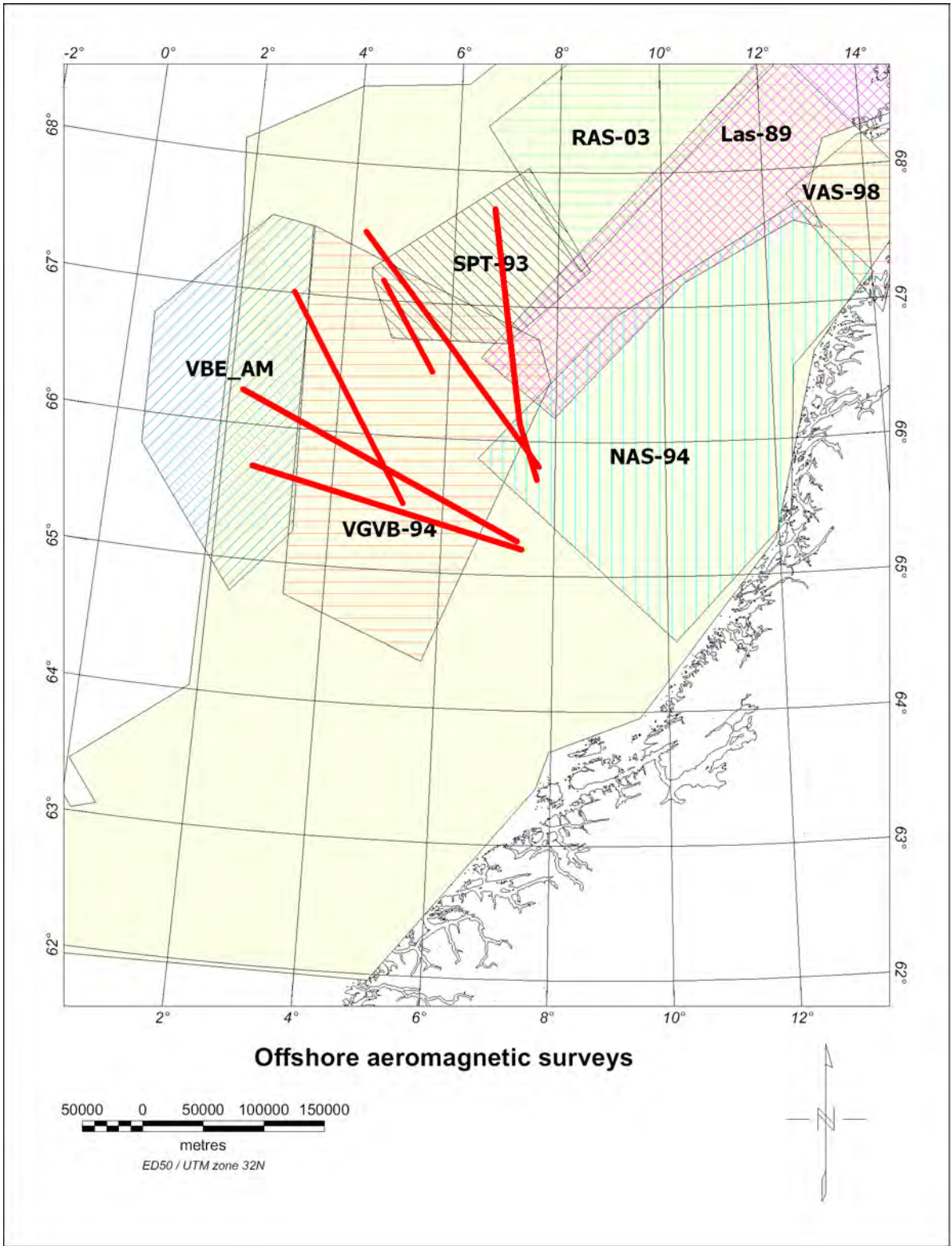


**Figure 5** Offshore aeromagnetic surveys. The light yellow area indicates the area of the old surveys NGU-69, NGU-73 and NRL-73.

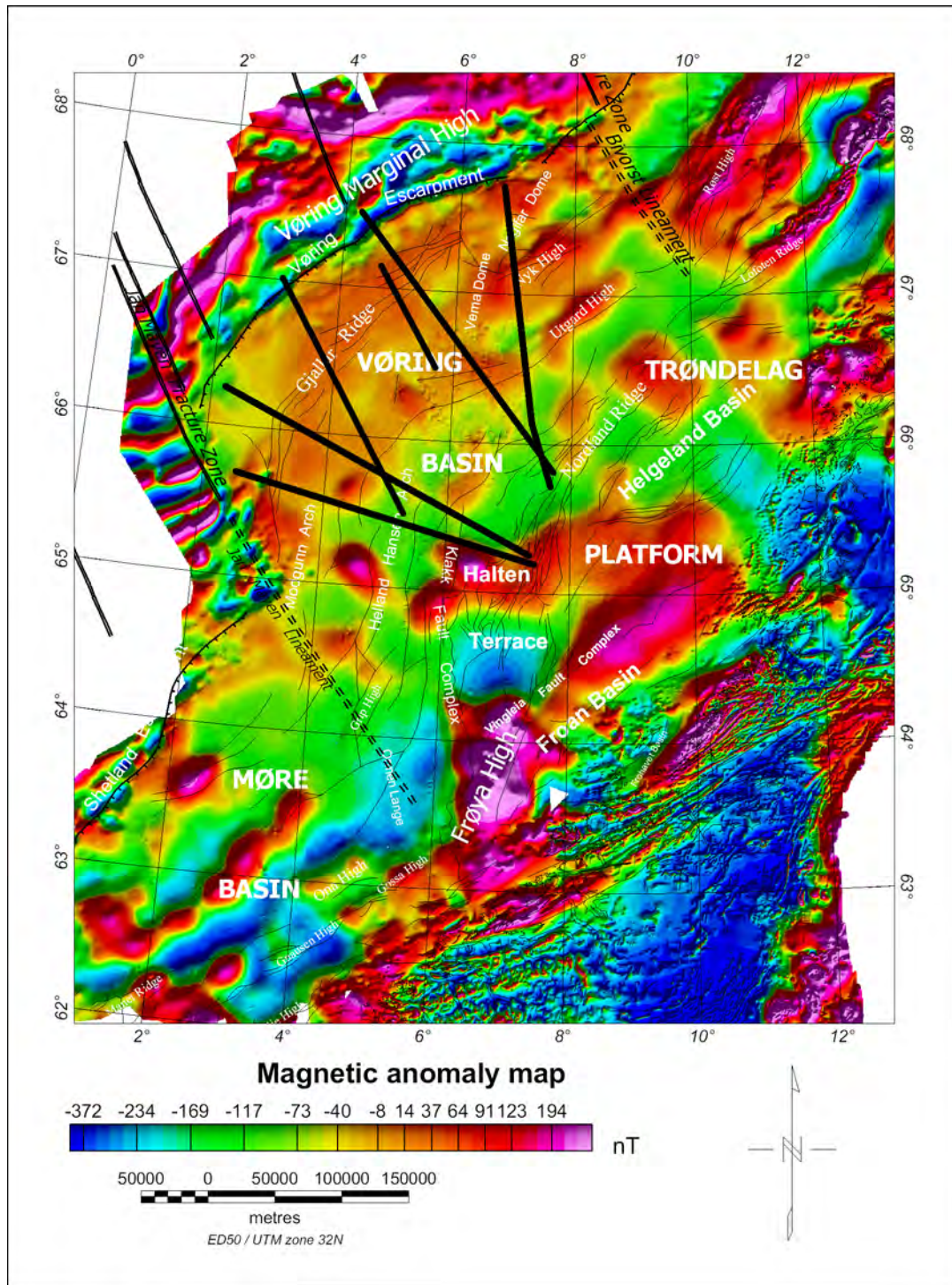


**Figure 6** Total magnetic field referred to DGRF on the Mid-Norwegian continental shelf. See text for data description.

### 3.4 Bathymetric data

The bathymetric data (Figure 7) were used to process the gravity data and to constrain the water depth in the modelling process. The data are taken from a compilation by Dehls et al. (2000). In the study area the water depths decrease from the west to the east towards the Trøndelag Platform; the profiles are located within the continental shelf and do not cross into the deep oceanic basin.

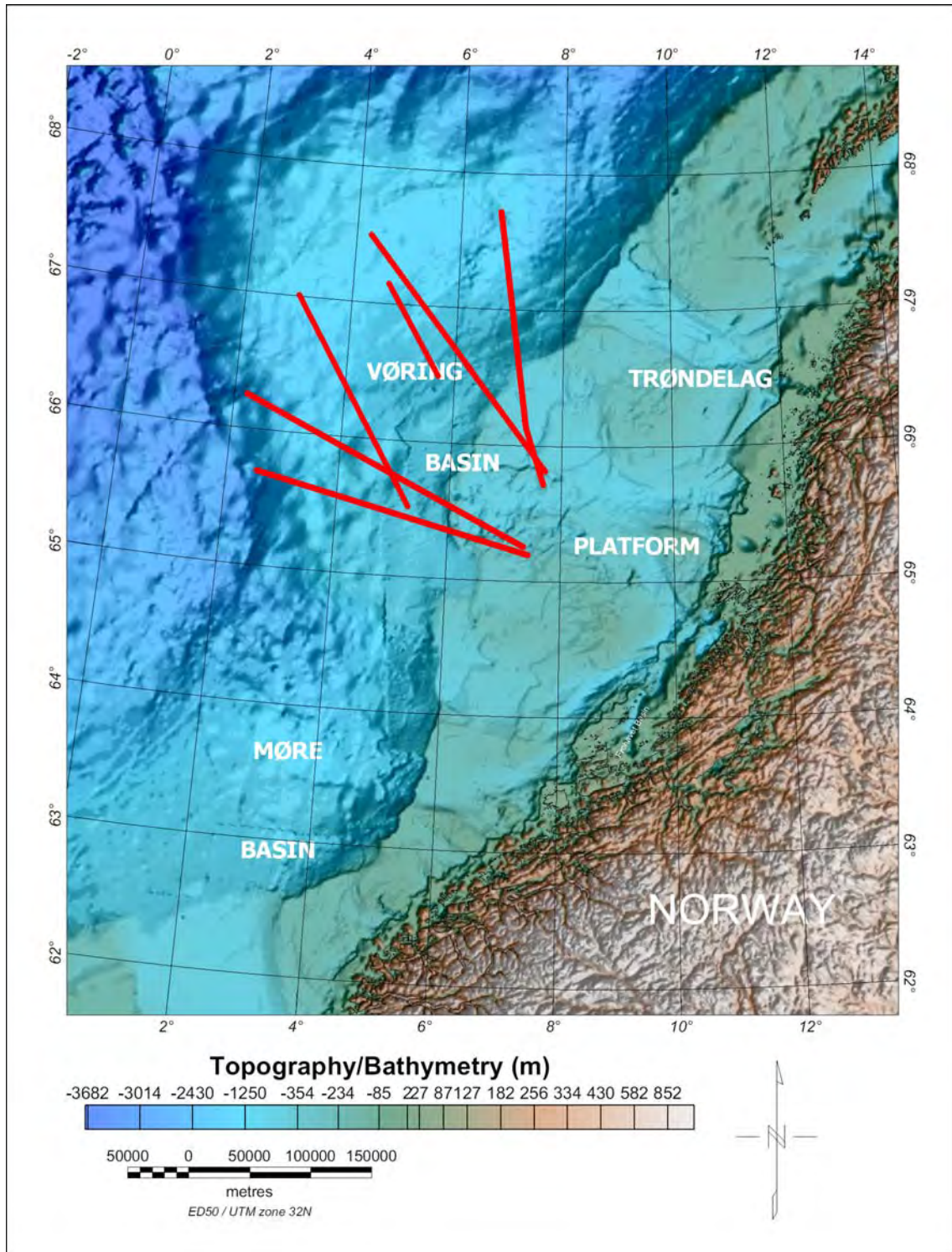


**Figure 7** Bathymetry/topography of the Mid-Norwegian Shelf and the adjacent mainland (after Dehls et al. 2000).

### 3.5 Density information

The two parameters most important for constructing the 3D density model are the geometry and the density of the structures. The densities used in the model process are based on published values (Raum et al. 2002, Mjelde et al. 2001, Mjelde et al. 1998, Olesen et al. 2002, Olesen and Smethurst 1995, Trinidad 2003). The densities in these studies are based on different sources as velocity-density relationships (e.g. Ludwig et al. 1970) or density logs of exploration wells on the Nordland Ridge and Utgard High (e.g. Olesen et al., 2002). The values in this study are consistent with the previous works (see Table 5).

	Raum et al. 2002	Mjelde et al. 2001	Mjelde et al. 1998	Olesen et al. 2002	Olesen & Smethurst 1995	Trinidad 2003	<i>this study</i>
Water	1030	1030	1030	1030	1030	1030	1030
Tertiary				2200	2200	2150	
Upper Tertiary /Neogene	1950-2150					2140	1950-2150
Lower Tertiary	2250						2200
Cenozoic Sediments	2200-2380	1900-2150	1950-2200				
Cretaceous Sediments	2400-2650		2450-2670		2350		2350-2680
Upper Cretaceous				2350		2350	
Lower Cretaceous				2500		2450	
Pre Cretaceous	2680-2760	2700-2810	2830				2600-2700
Jurassic					2450	2580-2670	
Triassic				2580	2580	2600-2690	
Paleozoic					2580	2600-2700	
Lower Volcanics /Sills		2620-2800					
Upper Volcanics		2700-2770					
Cont. Crust	2820-2840	2820-2900	2700-2950	2750-2950	2750	2700-2900	2750-2950
Oceanic Crust		2850-3020		2800-3000			2800-2950
Magmatic Underplating	3000-3120	3110-3220	3100-3230	3100			3100
Mantle	3300-3340	3330-3360	3330	3250	3300	3100-3300	3330

**Table 5** Overview of reported densities of geological units on the Mid-Norwegian continental margin. Density values in kg/m<sup>3</sup>.

In addition to the density structure of the crust (as described below) the lithospheric mantle was modelled by assuming a stepwise increase (200 K) in temperature from the Moho (c. 500°C) to the asthenosphere at a temperature of c. 1300 °C. Therefore a thermal expansion factor of  $3.2 \times 10^{-5} \text{ K}^{-1}$  was applied, adapted from studies by Breivik et al. (1999) for the Barents Sea and from Olesen et al. (2002) for the Nordland offshore area.



## 4 FORWARD MODELLING

Forward modelling of the gravity and magnetic fields has been done with the modelling software IGMAS (Interactive Gravity and Magnetic Application Software: Götze and Lahmeyer 1988, Schmidt and Götze 1998, Breunig et al. 2000). The software is used for the 2D and the 3D modelling.

The depth-converted interpretations from BP along the seismic profiles were used to construct initial 2D density models. We tried to achieve a solution utilizing the information from the other studies listed above. The models were consequently highly constrained by the additional information. In two cases the models had to be extended to 3D density models to give a reasonable adjustment to the observed gravity field. To avoid edge effects the models are extended 5000 km in each direction.

### 4.1 Profile GVLO

In Figure 8 the interpreted 2D density structure along the profile GVLO is presented. This profile intersects, as mentioned above, three of the OBS lines published by Raum et al. (2002). The modelled gravity response shows only minor misfits to the measured free-air gravity. Geometries and densities are mainly based on the information described above and only minor adjustment had to be made to these parameters to allow a good fit of the model to the measured gravity. Two main sources affect the gravity response: (1) depth to the Moho and (2) existence of magmatic underplated material. In the northwestern part of the model, from the Vøring Escarpment to the Slettringen Ridge, the Moho has a depth of 15 to 18 km and is buried by 2-4 km of underplated magmatic material. The magmatic underplating is well constrained by the OBS-cross lines.

The depth to the Moho increases to 22 km in the south-eastern part of the model below the Helland-Hansen Arch, the Rås Basin and the Halten Terrace and the magmatic underplated material is replaced by lower crustal material with slightly higher density ( $2950 \text{ kg/m}^3$ ) than the middle and upper crust ( $2850 \text{ kg/m}^3$  and  $2700 \text{ kg/m}^3$ , respectively).

In addition to the deep crustal features, the depth of the sedimentary basin strongly affects the gravity field. The main changes in the gravity field along the profile correlate well with the thickness of the sediments. The basin geometry is well constrained by the reflection seismic data. However, two features are noticeable and not unambiguously resolved by the seismic information. First, northwest and below the Gjallar Ridge (or Rån Ridge as named by Gernignon et al. 2003) a thick sedimentary body has to be introduced, below the Cretaceous sedimentary sequences. The OBS cross-line indicates such a structure, which originally was not present in the BP interpretation. First, the pre-Cretaceous structure is not unreasonable and it is necessary to fit the calculated gravity to the observed gravity field. Second, there is a need for a local updoming of the Moho between km 50 and 80, below the transition from the Gjallar Ridge to the Vigrid Syncline. This area is poorly constrained by all the seismic results and therefore the updoming is in agreement with the available information. However, the

tectonic implications of this structure have to be considered in further investigations. Along profile GVLO the conversion from seismic information to the density model is simple. In the interpretation of BP, no key structures are missing that would have a significant influence on the gravity field. The depth to the base Cretaceous is approx. 10 km and the total thickness of the sediments is around 10 km in this interpretation. Below the base Cretaceous a strong, elongated reflector is visible in the seismic sections. This reflector is interpreted as the top of the underplated body and/or intracrustal reflectors.

An alternative model was made to test a possible depth of the base Cretaceous of 14 to 15 km. This interpretation assumed that the deep strong reflectors are connected to the base Cretaceous. Figure 9 shows the model result based on this interpretation. The fit between modelled and measured free-air gravity is not as good, and further changes in geometries and densities of the model would be necessary. However, the needed changes would be in disagreement with the geologic and seismic knowledge and are hard to explain. For example the sedimentary unit would have a thickness of 14 km and would lie directly on the lower crust or on the underplated magmatic body. A body of high density ( $> 3000 \text{ kg/m}^3$ ) is needed to give a reasonable fit with the gravity field. As a consequence, any crustal layer is missing here. In the central part of the model, below the Helland Hansen Arch, more masses have to be included to shift the modelled anomaly to the level of the observed anomaly. However, the thick sedimentary unit with its relatively low densities makes it difficult to include more masses in the model. A change of the geometries of the deeper parts is inconsistent with the results of the OBS lines. The modelling shows that in case of a 14 km deep sedimentary basin, further structural changes must be considered which cannot be supported. Therefore, it is most likely that the deep reflectors indicate (a) the top of magmatic underplating and (b) intracrustal reflectors.

## 4.2 Profile VMT

Profile VMT is located south of profile GVLO, about 50 km to the south at its western end, while the eastern endpoints almost coincide. Therefore, the main structural elements and features are similar to those described above. Figure 10 shows the 2D model along the profile. The model is able to explain the observed and modelled gravity effects with some minor misfits at the Klakk Fault and in the Modgunn Arch. These minor misfits are probably related to 3D effects. There are certain differences between the initial BP seismic interpretations, which constrain the starting geometry, and the density model. Therefore, changes to the interpretation have been made in respect to the OBS data (Raum et al. 2002) and to adjust the gravity response of the model. A comparison with the reflection seismic data showed that the new geometry is in agreement with the revised interpretation (pers. com. E.K. Hansen).

The final geometry of the model shows a Moho depth of 17 to 18 km below the Gjallar Ridge and the Modgunn Arch. Below the Fles Fault Complex the Moho is at a depth of 16 km and again deepens to the east. The Moho upwelling below the Fles Fault Complex is not prominent, but is the boundary between the magmatic underplated material ( $3100 \text{ kg/m}^3$ ) to the west and

the lower continental crust ( $2950 \text{ kg/m}^3$ ) to the east. The small undulations in Moho geometry also cause a rather smooth gravity anomaly. The gravity anomaly is changing between -20 to +20 mGal with no steep gradients, which reflects the gentle changes of geometry along the profile. The basement/middle crust shows changes from 2800 to  $2950 \text{ kg/m}^3$ . The highest basement density occurs below the Fles Fault Complex and this can be related to the upwelling of the Moho.

The depth to the basement is the second most important source for the gravity signal. Below the Gjallar Ridge the basement depth is 8 km, deepening to almost 12 km below the Modgunn Arch. From the Fles Fault Complex to the Klakk Fault the basement depth shallows from 10 km to only 5 km. Below the Halten Terrace the basement depth is around 5-6 km. Despite the changes in geometry the gravity anomaly changes only between -10 to +20 mGal.

### **4.3 Profile VBT94**

The central long profile intersects the seismic array published by Mjelde et al. 1997 and is next to the OBS lines by Mjelde et al. 2001 (Figure 2).

#### **4.3.1 2D density model**

Figure 11 shows the results of the modelling. The gravity effect of the model does not completely fit the measured free-air gravity. Below the Fenris Graben and Gjallar Ridge the model shows a deviation from the measured field that cannot be matched with the given constraining information. In addition to this misfit the central part of the model, below the Vigrid Syncline and Fles Fault Complex, shows rather high crustal densities. These densities are at the upper limit for crustal densities and are more likely for lower crustal material.

The free-air gravity field (Figure 4) shows that the profile VBT94 is located in an area of strong lateral gravity changes perpendicular to the profile orientation. These changes relate to the Utgard High and the Nyk High north of the profile, affecting the Gjallar Ridge and Vigrid Syncline along the profile. To consider the masses outside the profile a 3D model is needed. In the area of profile VBT94 detailed information is available, which allows us to construct a 3D model.

The seismic profile GVF is located around 20 km to the south of profile VBT94, and is almost parallel to it. In addition the seismic OBS network by Mjelde et al. (2001) is covering the whole area and provides constraints on the regional structure, especially to the north of profile VBT94.

#### **4.3.2 3D density model - Profiles VBT94 and GVF**

The 3D density modelling was carried out in the area of profile VBT94 and consists of three interpreted cross-sections. The central profile is located along profile VBT94. The other two are parallel but shifted c. 25 km to the north and south of the main profile (see Figure 2 for

exact location). The southern profile correlates roughly with the seismic profile GVF and OBS line 4 in Mjelde et al. 1997. The northern profile corresponds roughly with the OBS line 7 in Mjelde et al. 1997 and is located close to the Surt Lineament. The results from the seismic studies constrain the 3D model and make the results more reliable. Figures 12-14 present the interpreted cross-sections of the 3D model. The model shows a good correspondence between the measured and modelled free-air anomaly along all three model sections, but the geometries of the three sections vary considerably.

The southernmost profile GVF (Figure 12) is dominated by a -20 mGal gravity low below the Gjallar Ridge and Vigrid Syncline and an increase to a level of +20 mGal to the southeast of the Fles Fault Complex. The gravity low corresponds to a thick sedimentary sequence with Tertiary, Cretaceous and thick pre-Cretaceous sediments. To the southeast the water depth is shallower and the Neogene thickness increases in the Rås Basin. Below the Fles Fault Complex a Cretaceous fault is observed, which at depth terminates near the southeast border of the magmatic underplated body. The magmatic underplated material has a maximum thickness of 8 km.

The profile VBT94 shows a generally similar picture (Figure 13). There are two sedimentary basins, the Gjallar Ridge-Vigrid Syncline and the Rås Basin, divided by a Cretaceous fault - the Fles Fault Complex. The northwestern sedimentary package extends to a depth of 12 km, while the sediments in the Rås Basin reach a depth of 14.5 km. The strong reflectors below the sedimentary structures are interpreted to partly correlate with the top underplating, but in other cases to be intra-crustal reflectors.

The northernmost profile (Figure 14) is particularly interesting in its northwestern part. Below the Fenris Graben, the Gjallar Ridge and the Vema Dome lie very thick Tertiary and pre-Cretaceous sediments in the model. Below the Gjallar Ridge the magmatic underplated body shows additional updoming of a few kilometres, which also affects the geometry of the sediments. The thickness of the sediments and the updomed magmatic underplated body are constrained by the OBS lines. The magmatic updoming is shifted 20 km south-eastwards compared with the Moho updoming. A local maximum is observed in the gravity field, clearly correlating to the updoming. At the transition from the Vigrid Syncline to the Rås Basin the free-air gravity shows an even stronger high, which also correlates in depth with a Moho updoming. Here the Moho updoming creates a boundary between the magmatic underplating and the lower continental crust. The geometry along the northern profile is showing some different features compared to the two other profiles and has a strong influence on profile VBT94, which is the reason for the misfits in the 2D modelling.

#### 4.4 Profile GRS

The results of the seismic interpretation along profile GVF have been used to construct the 3D model. To consider the BP interpretation along profile GRS another 2D model has been constructed (Fig. 15). The modelled profile is extended from the area of the GRS results to the

south, crossing the profile GVLO south of the Fles Fault Complex. In general, the model confirms all the statements and observations of the southern 3D profile (Line GVF) and the profile GVLO (Fig. 8 and 12). Only one feature is remarkable. Below the Gjallar Ridge the basement and overlying sedimentary sequences both show updoming. The updoming of the basement causes the free-air gravity high of +40 mGal.

The modelled gravity response is not perfectly adjusted to the observed free-air gravity. The gravity map (Fig. 4) shows that lateral changes appear in the gravity signal close to the profile, which can only be considered by a 3D model. But because profile GRS intersects profile GVLO in the south and the seismic interpretations of BP are only available over the Gjallar Ridge, a 3D model would provide only minor new constraints for the region. Therefore, no 3D modelling was performed.

#### **4.5 Profile BPN**

The profile BPN is the last of the modelled profiles and the most problematic to model. First of all the profile is located in north-south direction in the eastern area of the Vøring Basin. A comparison to the structural map and the gravity map (Fig. 1 and 4) of the Vøring Basin shows that the profile is crossing the structural elements and the gravity anomalies (especially in the Hel Graben) not perpendicular to the main strike/gradient directions, but obliquely. This complicates the modelling of the gravity field on a single 2D line. Therefore, the modelling was directly performed in the 3D domain with two additional lines, located 20 km to the east and west of the reflection profile (Fig. 2).

Figure 16 shows the modelled cross-section along profile BPN. The adjustment between the modelled and observed gravity field is not perfect, especially below the Naglfar Dome and at the transition between continental and oceanic crust. Below the Någrind Syncline and further to the south the modelled gravity effect fits the observed gravity quite well.

The misfit at the transition between oceanic and continental crust can be related to volcanic material, which could be emplaced in between the upper sediments, but also in the basement material. Below the Någrind Syncline the model structure shows a very different shape of the sediments than in the original seismic interpretation. However, the development of a new structural model for the area has significantly improved the match (pers. com. E.K. Hansen). The OBS data by Mjelde et al. (1997) are also in general agreement with the modelled structure.

The gravity anomaly has a level of -20 mGal in the part north of the Fles Fault Complex and of +60 to +40 mGal south of it, indicating differences between the northern and southern part and correlating with the domains of magmatic underplating in the north and "normal" lower crust in the south. The southern part of the model (south of Fles Fault Complex) is identical with the structures of the 3D model VBT and the results therein (4.3.2, Fig. 12-14). But in the northern part, in the Hel Graben, some interesting new features are visible. The magmatic

underplated structure has a very undulatory upper surface, while the Moho is only gently changing. The upper surface of the magmatic material is sub-parallel to the upper surface of the basement. But the shape is not in agreement with the deep seismic reflections. This questions the origin of the reflections (see detailed discussion in Chapter 6).

It has to be mentioned that the modelling of the gravity field in the Nyk High is difficult and a certain shift between the modelled and observed gravity signal still exists. To give a more exact model fit a few disadvantages have to be overcome and considered. First, the quality of the bathymetric data in the Hel Graben is not very good. Second, the quality of the OBS results is questionable in this area as the comparison to the reflection seismic results shows major differences. Third and probably most important, the location of the profile is not ideal to model the changes in the main geological features and in a related way, in the gravity field.

#### **4.6 Basement and Moho depth**

The results of the modelling allow construction of new depth maps of the Basement and Moho for the Mid-Norwegian Continental Shelf (Figures 17 and 18). Both maps are based on the results of the 2D- and 3D-modelling, but are in addition constrained by several previous studies.

The estimate of the offshore basement depth is based on studies by Olesen and Smethurst (1995), Olesen et al. (1997), Doré et al. (1999), Brekke (2000), Skilbrei and Olesen (2001), Olesen et al. (2002), Osmundsen et al. (2002), Skilbrei et al. (2002).

The Moho map is additionally based on the OBS results and the depth published by Kinck et al. (1993). Further input comes from the studies carried out in the BAT-project (e.g. Olesen et al. 2002, Skilbrei et al. 2002). The combination of all these results leads to highly constrained depth maps. The correlation between the structural elements, bathymetry and the Moho depth is obvious (compare Fig. 1, 7 and 18).

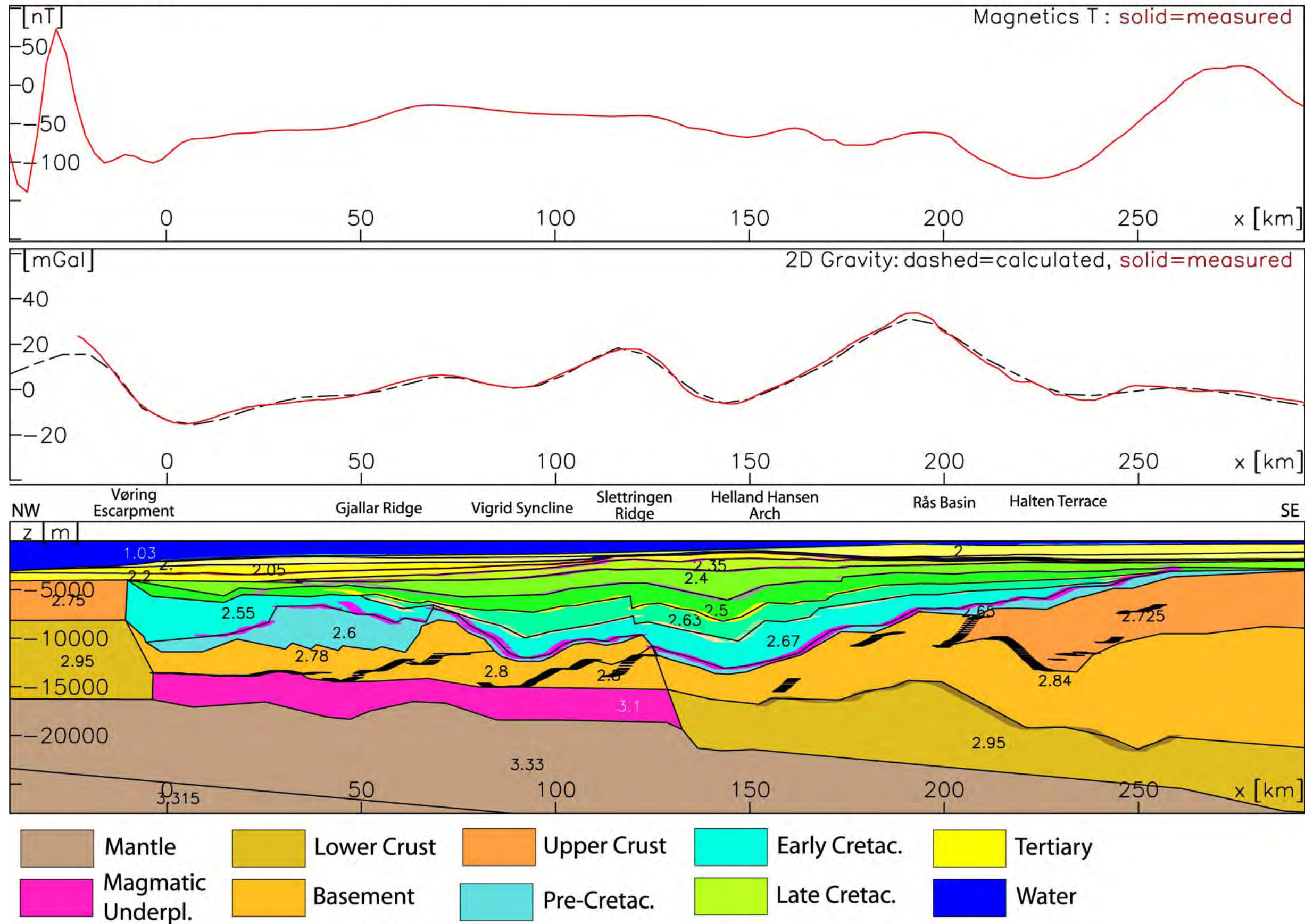


Figure 8 **Profile GVLO - 2D density structure, free-air-anomaly and magnetic anomaly.** The central part of the figure shows the measured (red) and calculated (dotted black) free-air gravity along the profile GVLO. The upper part shows the measured magnetic anomaly. The lower part shows the 2D density structure with an overlay of the interpreted seismic reflections by BP (coloured lines). The densities are in  $\text{g/cm}^3$  and the vertical exaggeration of the depth section is 2.5.



Deep reflectors= Base Cretaceous

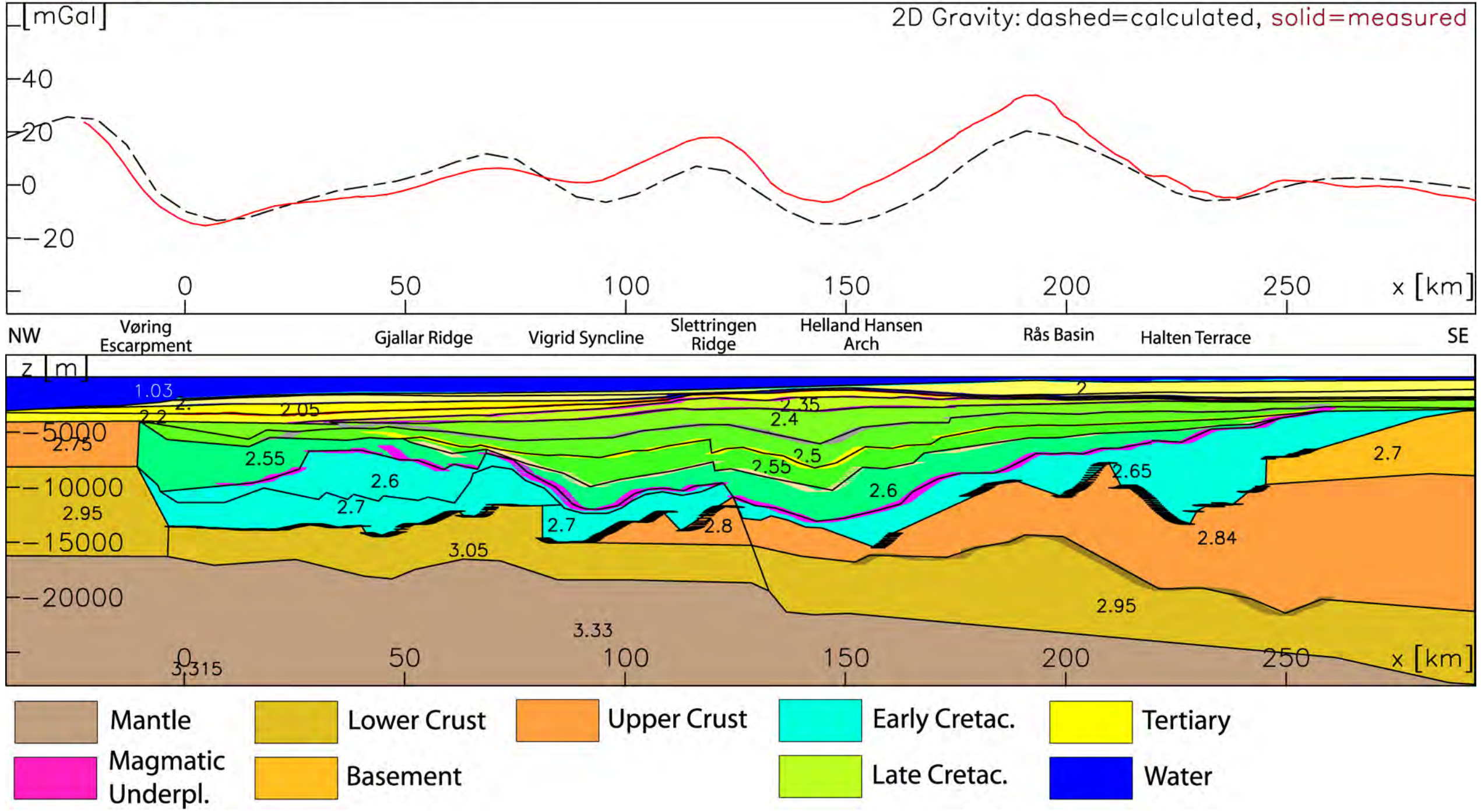


Figure 9 Profile GVLO - Alternative interpretation. In this interpretation the deep reflections have been interpreted as the base Cretaceous. Certain adjustments have been made to the model, but to give a reasonably good fit further adjustments must be made, for which we have no geophysical evidence. The upper part of the figure shows the measured (red) and calculated (dotted black) free-air gravity along the profile. The lower part shows the 2D density structure with an overlay of the interpreted seismic reflections by BP (coloured lines). The densities are in g/cm<sup>3</sup> and the vertical exaggeration of the depth section is 2.5.





3-D Gravity and Magnetic Modeling  
VMT

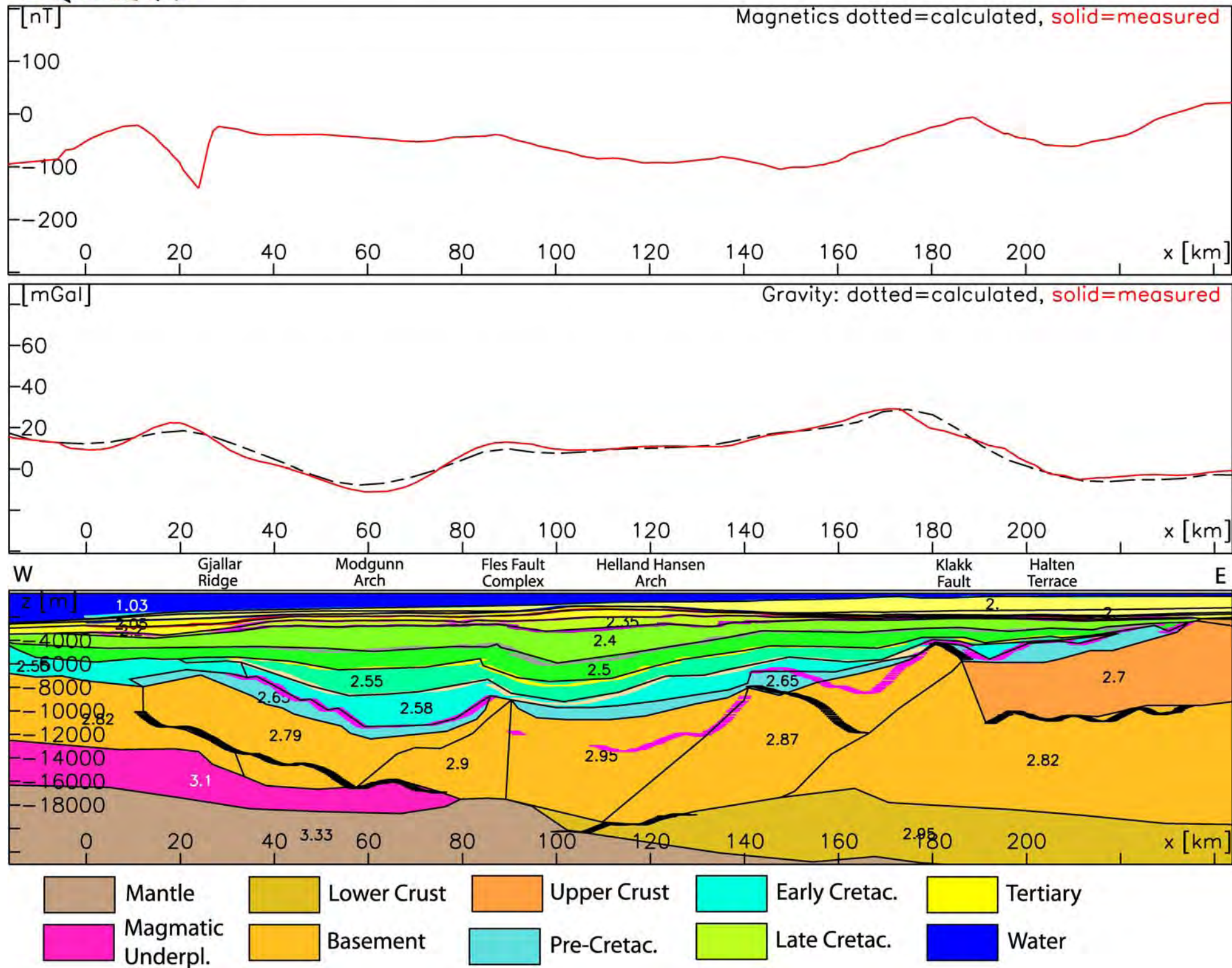


Figure 10 **Profile VMT - 2D density structure, free-air-Anomaly and magnetic anomaly.** The central part of the figure shows the measured (red) and calculated (dotted black) free-air gravity along the profile VMT. The upper part shows the measured magnetic anomaly. The lower part shows the 2D density structure with an overlay of the interpreted seismic reflections by BP (coloured lines). The densities are in  $\text{g/cm}^3$  and the vertical exaggeration of the depth section is 2.5.

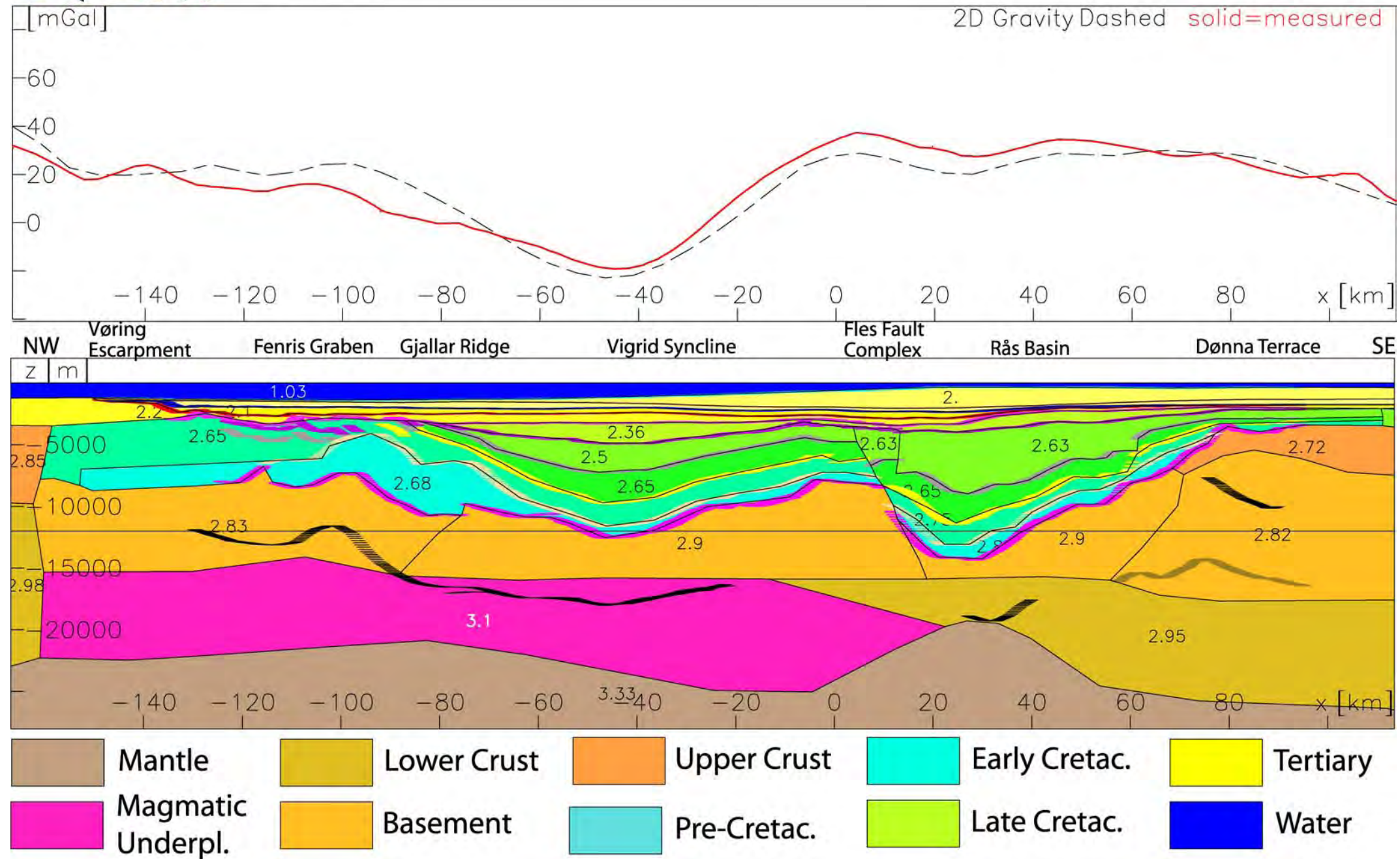
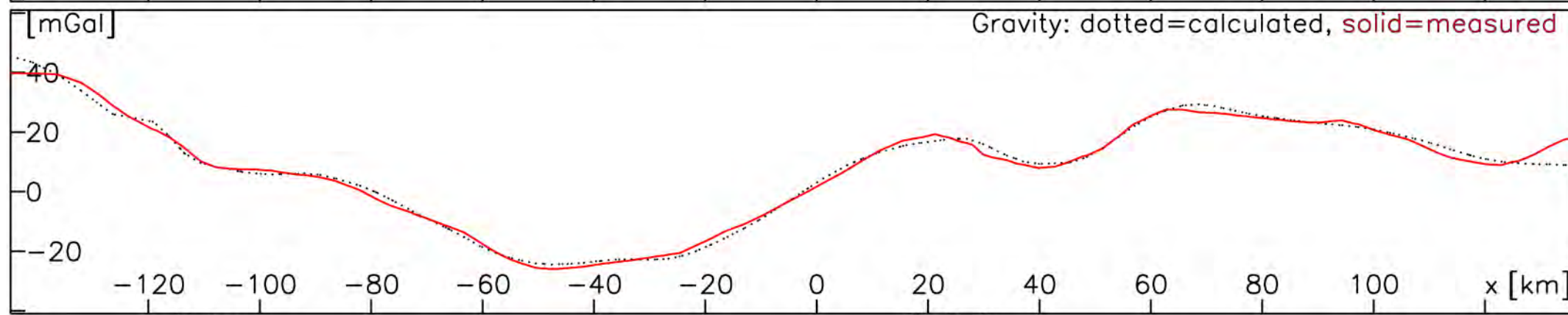
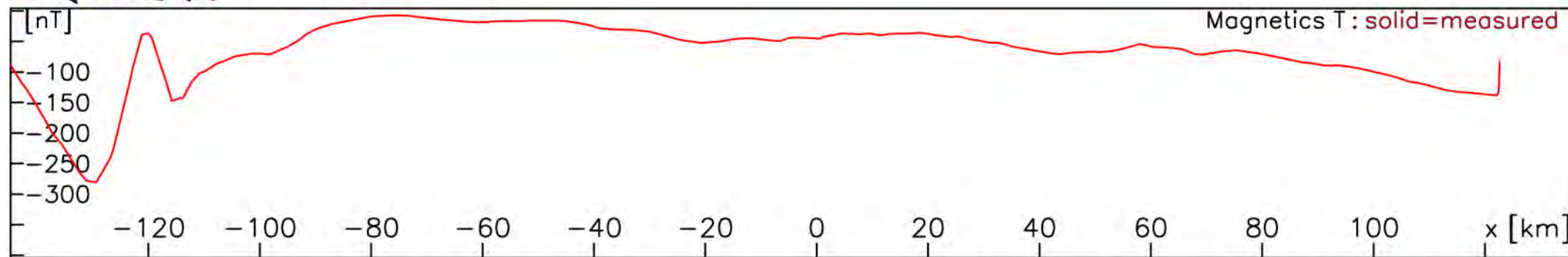


Figure 11 **Profile VBT 94 - 2D density structure and free-air-Anomaly.** A better fit between modelled and observed gravity could not be achieved with the seismic constraints in a 2D model. The profile is located in an area where the gravity field strongly changes perpendicular to the model section (see Fig. 4). The central part of the figure shows the measured (red) and calculated (dotted black) free-air gravity along the profile. The upper part shows the measured magnetic anomaly. In the lower part the 2D density structure and, as an overlay, the interpreted seismic reflections by BP (coloured lines), are shown. The densities are in  $g/cm^3$  and the vertical exaggeration of the depth section is 2.5.



NW Vøring Escarpment Gjallar Ridge Vigrid Syncline Fles Fault Complex Rås Basin Halten Terrace SE

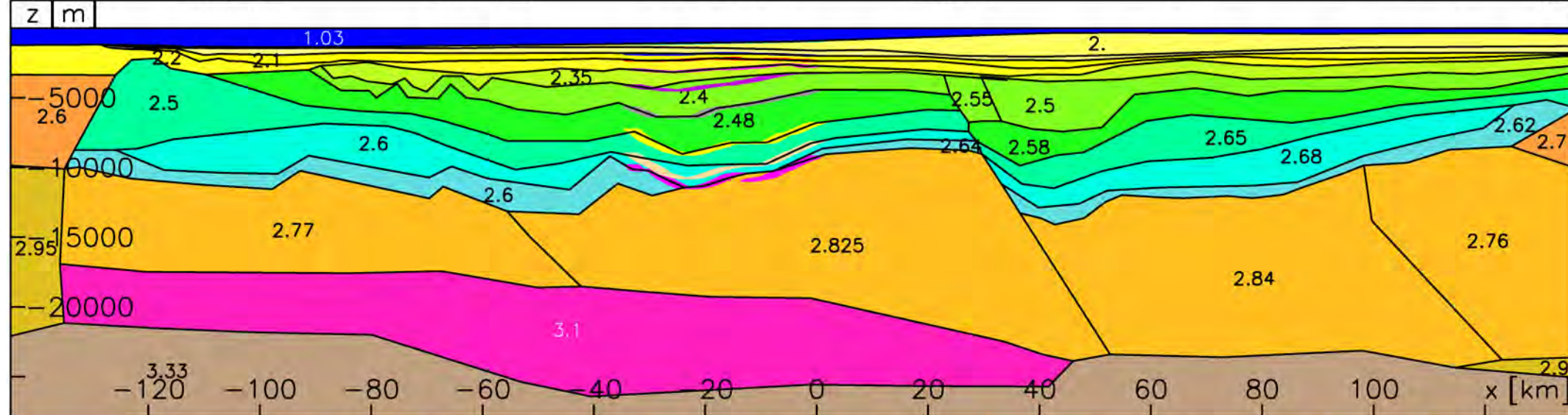
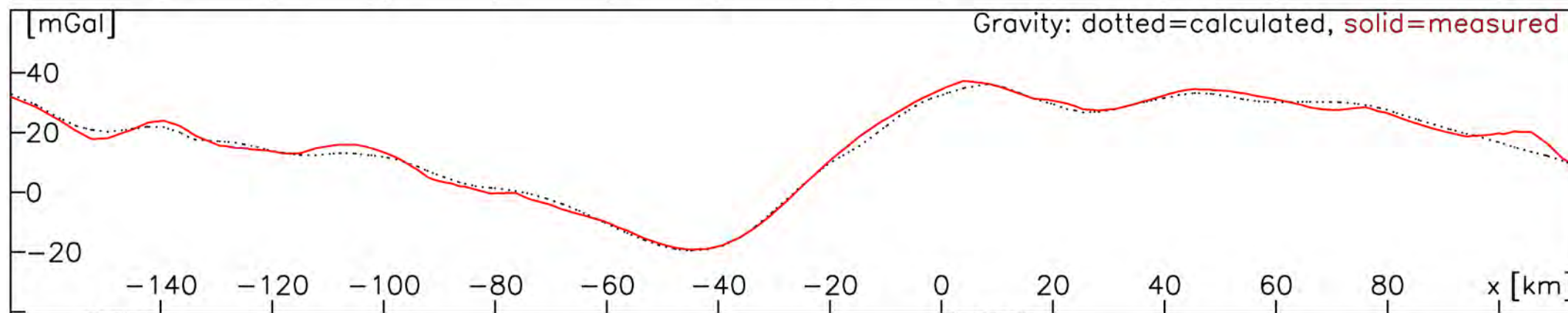
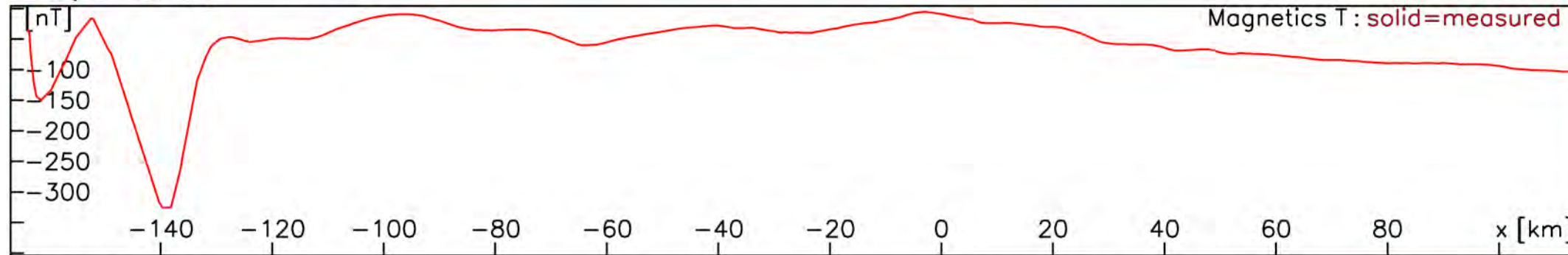


Figure 12 **The 3D model VBT94 - Southern cross section.** The cross section is near to line GVF and in a distance of app. 25 km to the south of line VBT94. The central part of the figure shows the measured (red) and calculated (dotted black) free-air gravity along the profile. The upper part shows the measured magnetic anomaly. The lower part shows the density structure with an overlay of the interpreted seismic reflections of line GVF by BP (coloured lines). The densities are in  $g/cm^3$  and the vertical exaggeration of the depth section is 2.5.



3-D Gravity and Magnetic Modeling  
3D-VBT94

Plane VBT94



NW Vøring Escarpment Fenris Graben Gjallar Ridge Vigrid Syncline Fles Fault Complex Rås Basin Dønna Terrace SE

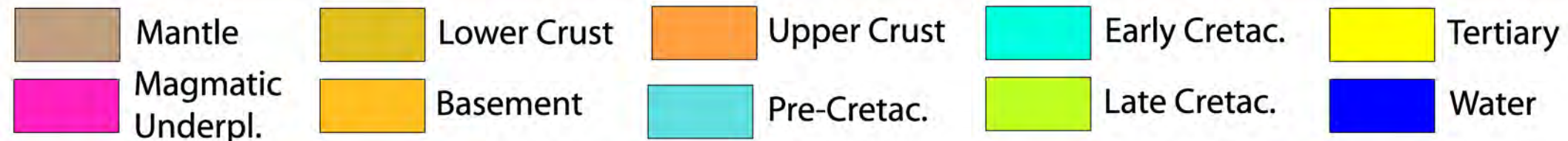
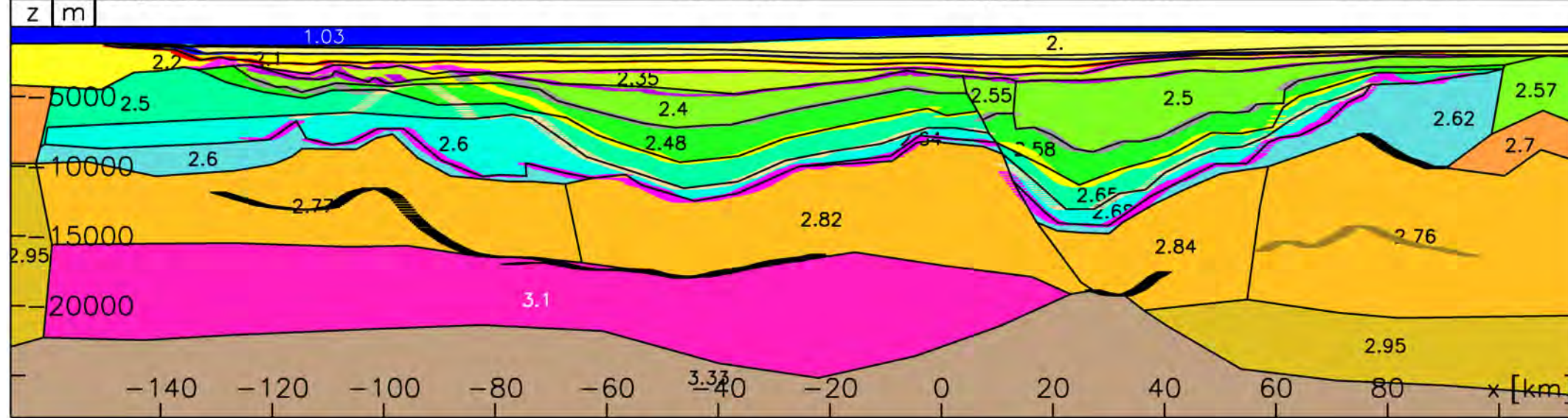
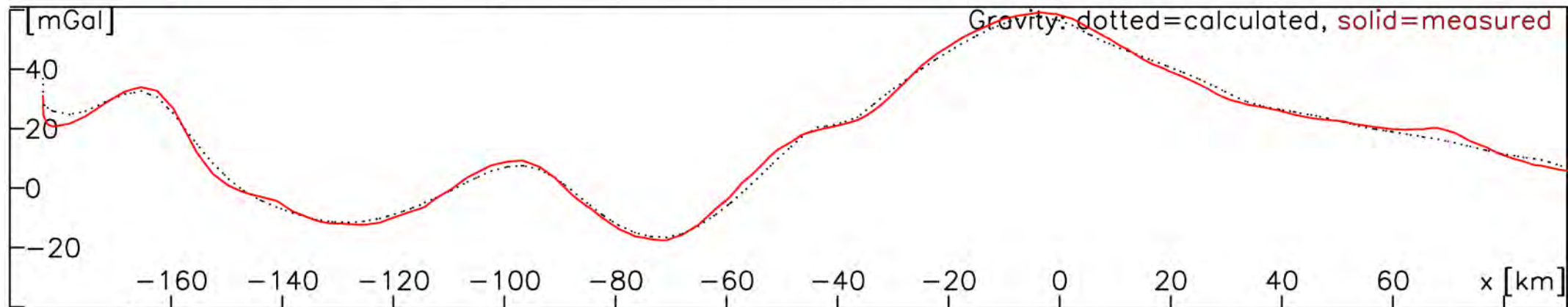
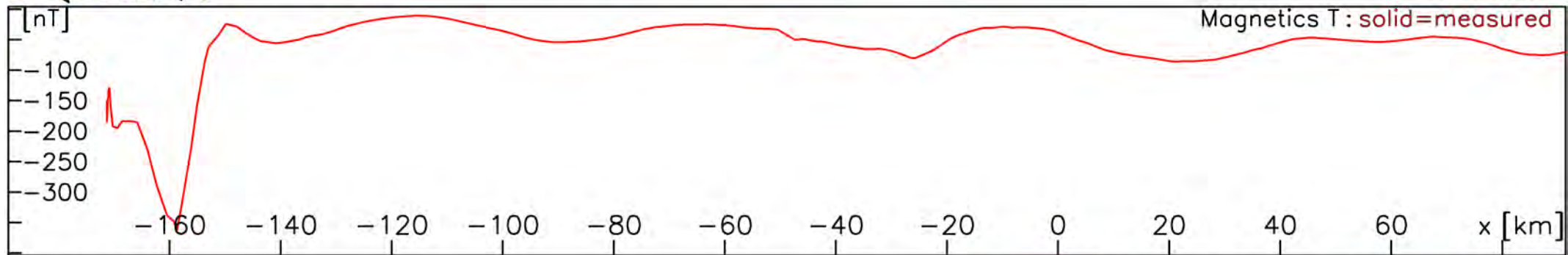


Figure 13 **The 3D model VBT94 - Central cross section.** The central cross section of the model is identically with the location of line VBT94. The central part of the figure shows the measured (red) and calculated (dotted black) free-air gravity along the profile. The upper part shows the measured magnetic anomaly. The lower part shows the density structure and, as an overlay, the interpreted seismic reflections of line VBT94 by BP (coloured lines), are shown. The densities are in  $g/cm^3$  and the vertical exaggeration of the depth section is 2.5.



3-D Gravity and Magnetic Modeling  
3D-VBT94

Plane North



NW Vøring Escarpment Fenris Graben Gjallar Ridge Vema Dome Vigrid Syncline Rås Basin Dønna Terrace SE

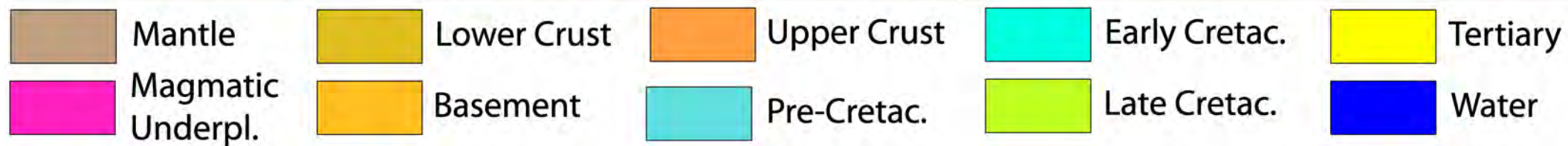
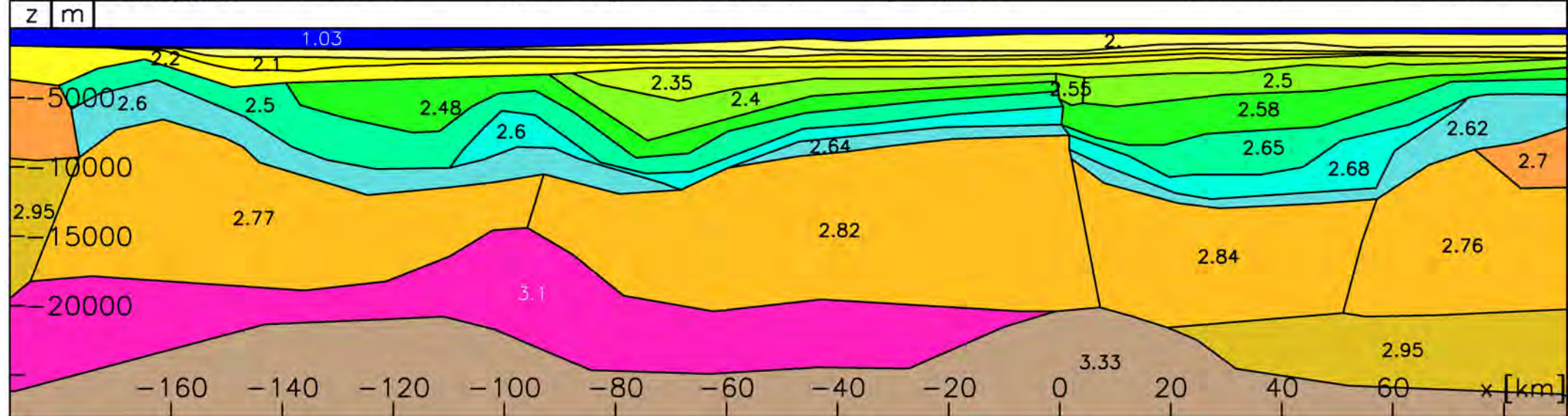


Figure 14 **The 3D model VBT94 - Northern cross section.** The cross section is a distance of app. 25 km to the north of line VBT94. The main constraints for the modelling of the line are the results of the OBS experiments by Mjelde et al. (1997). The central part of the figure shows the measured (red) and calculated (dotted black) free-air gravity along the profile. The upper part shows the measured magnetic anomaly. The lower part shows the density structure. The densities are in  $\text{g/cm}^3$  and the vertical exaggeration of the depth section is 2.5.



3-D Gravity and Magnetic Modeling  
GRS

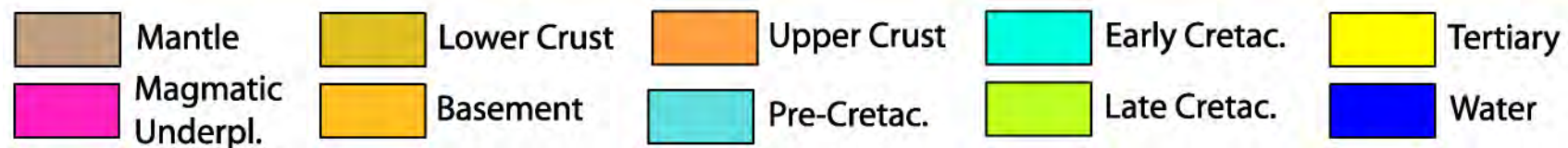
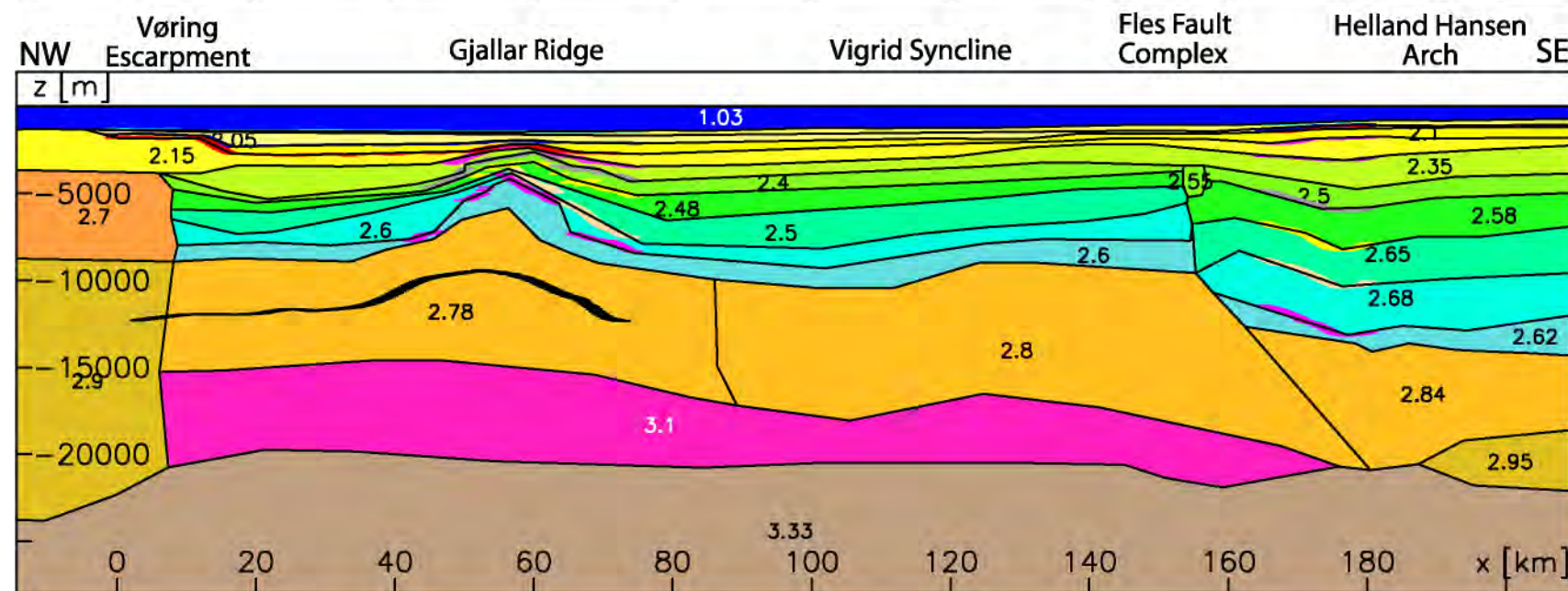
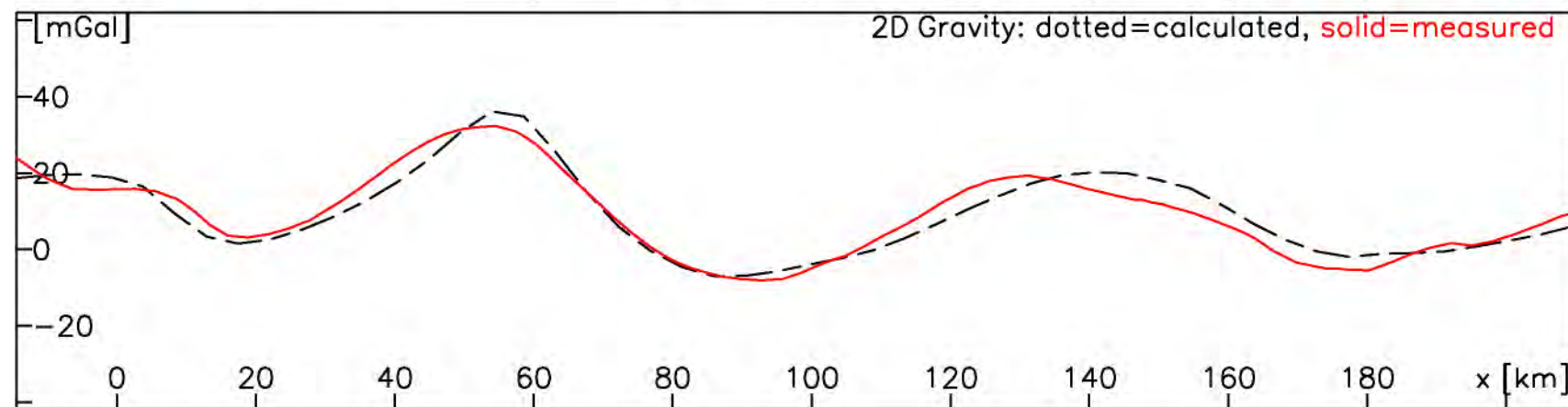
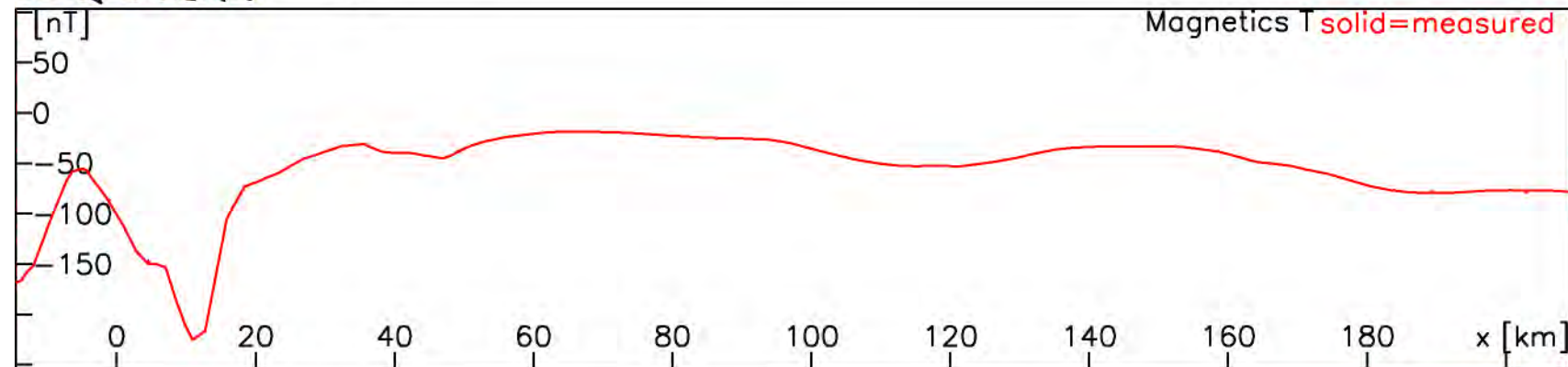


Figure 15 **Profile GRS - 2D density structure, Free-Air-Anomaly and Magnetic Anomaly.** The central part of the figure shows the measured (red) and calculated (dotted black) Free-Air gravity along the profile GVLO. The upper part shows the measured magnetic anomaly. The lower part shows the 2D density structure with an overlay of the interpreted seismic reflections of GRS99-232 by BP (coloured lines). The densities are in  $g/cm^3$  and the vertical exaggeration of the depth section is 2.5. South to the Fles Fault Complex the cross-section is crossing the profile GVLO (Fig.8).

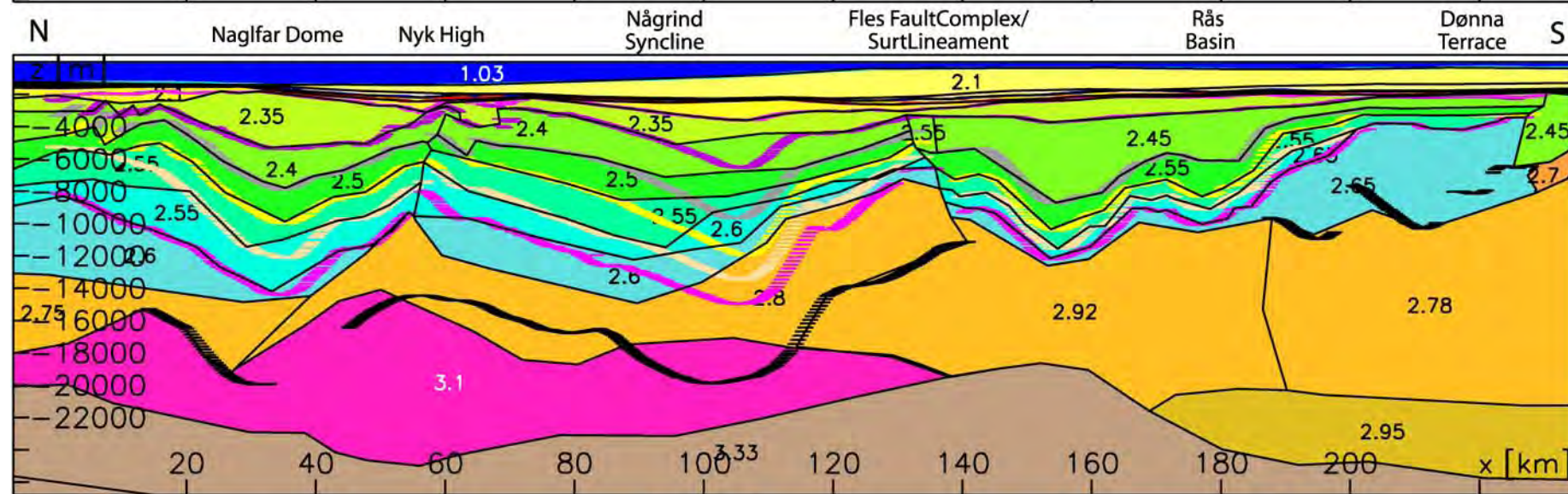
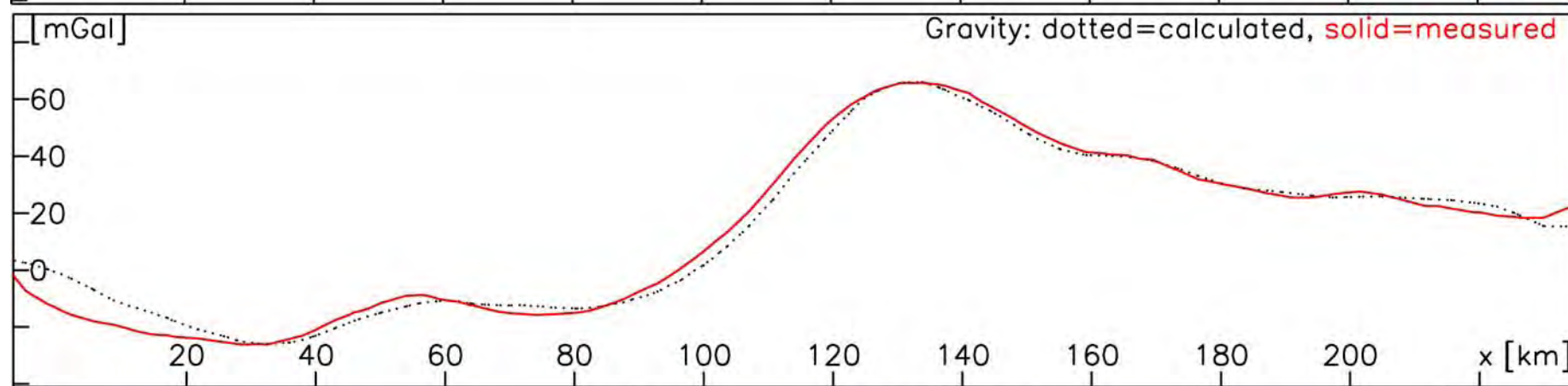
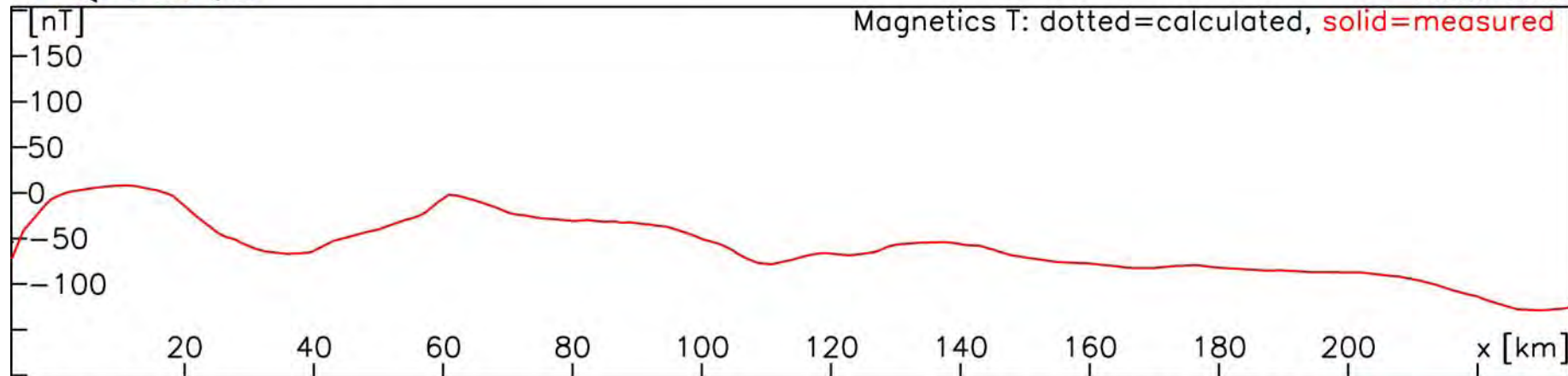
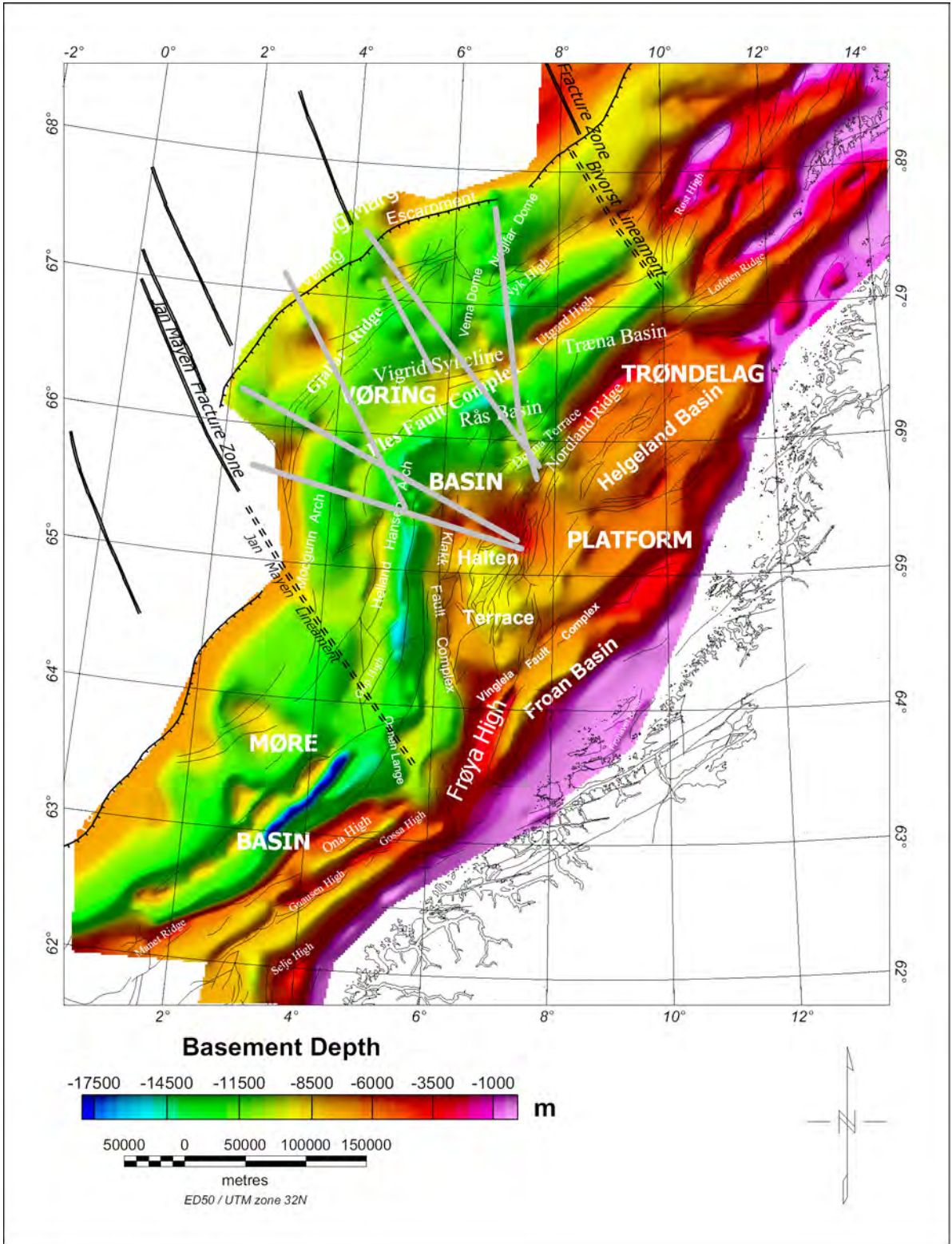


Figure 16 3D model BPN - density structure, free-air-anomaly and magnetic anomaly. The central part of the figure shows the measured (red) and calculated (dotted black) Free-Air gravity along the profile GVLO. The upper part shows the measured magnetic anomaly. The lower part shows the density structure with an overlay of the interpreted seismic reflections by BP (coloured lines). The densities are in  $g/cm^3$  and the vertical exaggeration of the depth section is 2.5.



**Figure 17** Basement depth on the Mid-Norwegian Continental shelf. See text for details.





## 5 MAGNETIC AND ISOSTATIC INTERPRETATION

### 5.1 Magnetic interpretation

The comparison of the gravity and magnetic maps shows that the main sources of the anomalies lie in different domains. To the landward side of the Vøring Escarpment the gravity (and magnetic) highs are related to the basement highs and intrusive rock complexes. The magnetic highs, however, correlate only partly with the gravity highs. But in general, the amplitude of the magnetic anomaly is very low along the interpreted profiles (Fig. 8, 10, 12-16). Only at the continent-ocean boundary (COB) is a prominent anomaly visible. Different studies have observed lava flows at the transition area, which are supposed to be highly magmatic and most likely the source of the major magnetic anomaly (e.g. Fichler et al. 1999, Osmundsen et al. 2002, Raum 2002).

The magnetic anomalies have not been modelled in this study, but compared to the modelled density structures along the profiles. The comparison indicates that a complete magnetic model has to include more detailed structures than the present models, especially in the range of the continent-ocean boundary. The more complex magnetic anomaly is resulting from possible intra-basement variations of magnetic attributes as well as intrusives (e.g. sills) encountered at shallower depths within the sediments (Fichler et al. 1999). But for a detailed modelling of the magnetic anomalies a lack of constraining information in these deep water domains has to be overcome. Further landwards from the COB the magnetic anomalies along the profiles show only minor undulations around  $-50\pm 50$  nT and correlate with the sedimentary structure. The presence of a shallow Curie isotherm may be a reason for this (Fichler et al. 1999). Close to the southeastern end of the profiles GVLO and VMT the magnetic anomaly shows a step of +200 nT (Fig. 6). The increase of the magnetic anomaly is correlating with the Nordland Ridge. In conclusion, the main magnetic anomalies are located outside the area of seismic results.

### 5.2 Isostatic implications

The isostatic state of the outer Vøring Basin was investigated by analysis along the profiles VBT94 and GVLO. These two models are the best constrained and represent the southern and central-northern Vøring Basin.

First, the loads along the profiles were calculated. The models are assumed to be close to isostatic equilibrium. With respect to a layered normal crust the loads at the crust-mantle boundary should be zero, if isostasy is complete in an Airy-type, or zero at a constant depth if the area is compensated in a Pratt-type of isostasy.

Figure 19 shows the relative loads along profile GVLO and VBT94. The loads are calculated within the models presented in 4.1.1 and 4.3.2. The results show that the area of profile VBT94 is close to isostatic equilibrium. The level of zero loads is near the crust-mantle boundary and has, in general, a good correlation with it. The small deviations can be due to

influence of the sub-crustal density structure. Along profile GVLO the zero level does not correlate as well with the Moho. Here the results indicate a constant depth of isostatic balance at 25 km depth. Here it seems that the area is compensated in the sense of a Pratt isostasy. Along both profiles the compensation depth is around 25 km and shows only undulations of  $\pm 2$  km, which is pointing to a Pratt type isostatic compensation of the outer Vøring Basin. However, a more detailed investigation of the isostatic state should take into account the regional setting of the Vøring Basin and its tectonic history.

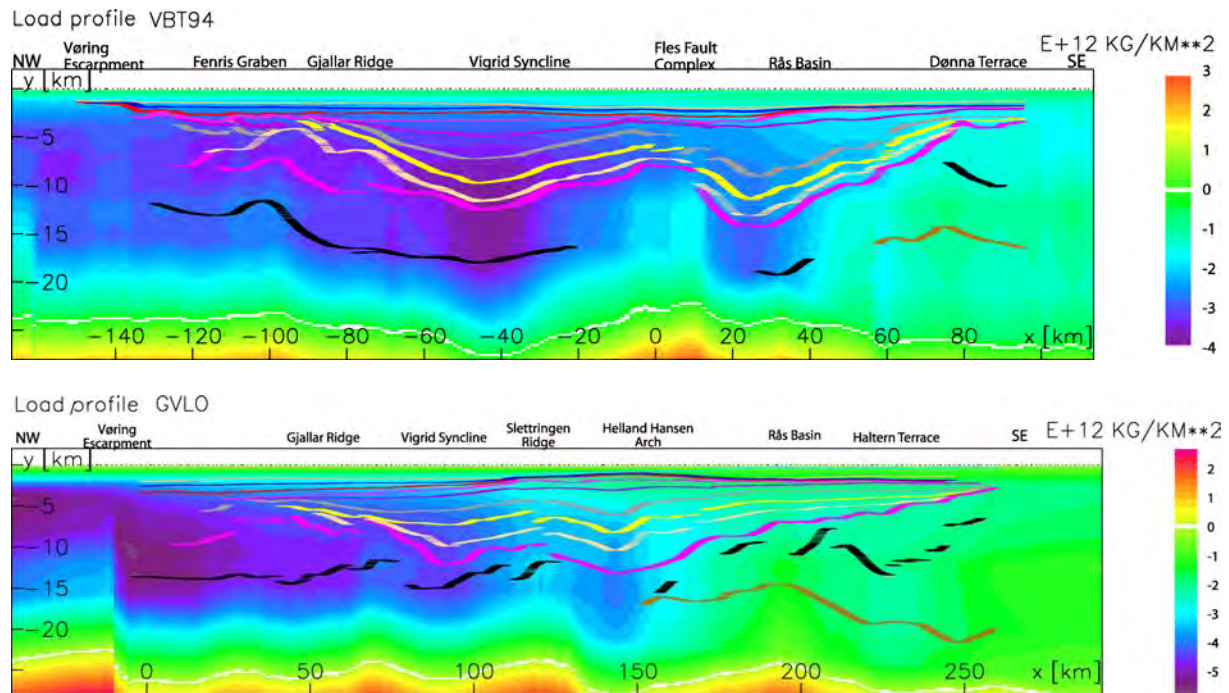


**Figure 19** Isostatic loads along the profiles VBT94 (top) and GVLO (bottom). The isostatic loads have been calculated by subtracting an isostatic reference density model from the actual density models in Figure 8 and 12. The white line is corresponding to zero loads, which is indicating the isostatic equilibrium surface.

## 1. 6 DISCUSSION AND INTERPRETATION

The variety of available information for the Vøring margin has allowed us to construct reasonable 2D-and 3D-models. The models show that the gravity field of the area is the result of the structure of the sedimentary basins and the geometry of the Moho together with the existence of magmatic underplated material.

While the magmatic underplated material and the density contrast at the Moho boundary generate a long wavelength anomaly pattern, the sedimentary basins are the source of long- to short wavelength anomalies. The overall thickness of the sediments is responsible for the long wavelength changes, while the internal geometry causes the intermediate to short wavelength changes. The geometry of the sediments is well constrained by the BP interpretation, but in the interpretation a certain amount of (Pre-Cretaceous?) sediments is missing. The sediments are affected by a variety of faults (e.g. Fles Fault Complex) that led to changes in sedimentary thickness giving rise to short wavelength anomalies.

The different density models have further shown that the base Cretaceous has a maximum depth of approx. 13 km. But for the deeper part of the profiles the BP interpretation shows some strong reflectors. These are probably not related to the sedimentary structures. A combination with OBS data indicates that these reflectors are partly caused by the top magmatic underplating and partly by intracrustal reflectors. There are different theories (e.g. Wheeler et al. 2002, Gernignon et al. 2003) about the origin of these reflectors. The present study cannot answer this question, but the results suggest a relationship with intrusion of sills in crust. Sills could cause the abrupt increases in velocity, with only minor increases in density values.

In this context, it is notable that the density within the basement has to be varied through the study area to give a reasonable fit to the observed gravity fields. These changes are clearly correlated with the visible surface structures and indicate a fragmentation into tectonic zones of the study area.

In addition to the interpretations, which are valid for the whole study area, certain differences exist between the profiles in the southern and central/northern Vøring Basin. The gravity field along profiles GVLO and VMT in the southern Vøring Basin can be reasonably fitted with a 2D model, as there are no strong lateral changes in the gravity field perpendicular to the profiles. Also the other results (e.g. OBS data) do not indicate major structural changes close to the profile location. In contrast, the gravity signal along the profiles VBT94 and BPN could not be successfully fitted by a simple 2D model. In the northwestern part of profile VBT94 the gravity signal is changing perpendicular to the cross-section. The change in the gravity is caused by an updoming of the Moho and the magmatic underplated body northeast of the profile, which is constrained by OBS results. To the south of profile VBT94, the sedimentary thickness increases and causes a gravity low. The updomed underplated body in the north and the increase of sediment thickness to the south strongly influence the gravity signal along profile VBT94. Similar problems are detected for profile BPN with the structural changes in the Hel Graben. Here an additional factor is the non-ideal location of the profile in relation to the geological structures.

An important difference between the northern and southern profiles is the Moho depth. Along profile VBT94 the Moho has a depth of approx. 22.5 km with a local minimum at a depth of 20 km below the Fles Fault Complex and Rås Basin area. This peak or Moho updoming is the transition between the occurrence of magmatic underplated material and lower continental crustal material.

Along profile GVLO the depth to Moho below the magmatic underplating is only at 16 km depth, deepening to the southeast to 20 km below the Rås Basin and deepening further outside the modelled area. The Moho is shallower along this profile and does not show any updoming. Isostatic investigations point to a similar compensation depth of around 25 km. In an isostatic interpretation the areas of the two profiles are compensated in the same way, but local differences exist. The local differences are important to consider in a tectonic

comparison/study of the area. Especially in a reconstruction of the Norway-Greenland rift the tectonic differences should be considered.

The shape of the magnetic field in the outer Vøring area suggests shallow sources at the COB, which are probably connected to igneous rocks, in contrast to the gravity field. A more detailed interpretation of the magnetic anomalies would require detailed magnetic modelling. The different sources of the gravity and magnetic signal would require new models, which focus more on the magnetic important sources, located outside the main seismic study areas. Therefore, such a task cannot be fulfilled with the information used in the present study.

The results of the density models show that there exist clear differences between the southern and central-northern Vøring Basin. To be able to further investigate these differences a 3D structural model of the whole Vøring Basin constrained by the OBS data and reflection seismic profiles would be useful. Such a model can give insights into the transition between the southern and central-northern Vøring Basin. A combination of the 3D model with results from the Møre Basin and the Lofoten/Nordland area would further enhance the quality of the results.

## **7 ACKNOWLEDGEMENTS**

The study was initiated and financed by BP Norway. Eirik Mauring and Odleiv Olesen processed the magnetic and gravity data. Evan Kåre Hansen (BP), Graham Yielding (Badleys) and Erik Lundin (NGU) gave advice and consultation during the interpretation.

## **8 REFERENCES**

- Andersen, O.B. and Knudsen, P., 1998. Gravity anomalies derived from the ERS-1 satellite altimetry. Kort og Martykelstyrelsen, Kopenhagen ([www.kms.dk](http://www.kms.dk)).
- Blystad, P., Brekke, H., Fjærsteh, R.B., Larsen, B.T., Skogseid, J. and Tørudbakken, B., 1995. Structural elements of the Norwegian continental shelf. Norwegian petroleum Directorate Bulletin, 8.
- Brekke, H., 2000. The tectonic evolution of the Norwegian Sea continental margin with emphasis on the Vøring and Møre basins. In: Nøttvedt, A. (ed.) Dynamics of the Norwegian Margin. Geological Society of London, Special Publication, 167, 327-378.
- Breivik, A.B., Verhoef, J. and Faleide, J.I., 1999. Effects of thermal contrasts on gravity modeling at passive margins: results from the western Barents Sea. JGR, 104, 15293-15311.
- Breunig, M., Cremers, A.B., Götze, H.-J., Schmidt, S., Seidemann, R., Shumilov, S. and Siehl, A., 2000: Geological Mapping based on 3D models using an Interoperable GIS. Geo-Information-Systems, Journal for Spatial Information and Decision Making, 13: 12-18.

Dehls, J.F., Olesen, O., Bungum, H., Hicks, E., Lindholm, C.D. & Riis, F., 2000. Neotectonic map, Norway and adjacent areas 1:3 mill. Norges geologiske undersøkelse, Trondheim, Norway.

Doré, A.G., Lundin, E.R., Jensen, L.N., Birkeland, Ø., Eliassen, P.E. and Fichler, C., 1999. Principal tectonic events in the evolution of the northwest European Atlantic margin. In: Fleet, A.J. and Boldy, S.A.R. (eds.) Petroleum Geology of Northwest Europe: Proceedings of the 5th conference, 41-61. Geological Society, London.

Eldholm, O. and Grue, K., 1994. North Atlantic volcanic margins; dimensions and production rates. *JGR*, B, 99, 2955-2968.

Fichler, C., Rundhovde, E., Olesen, O., Sæther, B.M., Rueslåtten, H., Lundin, E. and Doré, A.G., 1999. Regional tectonic interpretation of image enhanced gravity and magnetic data covering the Mid-Norwegian shelf and adjacent mainland. *Tectonophysics*, 306, 183-197.

Gernignion, L., Ringenbach, J.-C., Planke, S. and Le Gall, B., 2002. Crustal structure and rifting along volcanic rifted margins: the Vøring Margin (Mid-Norway). In: Jónsson, S.S. (Editor): 25th Nordic Geological Winter Meeting, Abstract Volume, 61.

Gernignion, L., Ringenbach, J.C., Planke, S., Le Gall, B. and Jonquet-Kolstø, H., 2003. Extension, crustal structure and magmatism at the outer Vøring Basin, Norwegian margin. *Journal of the Geological Society*, London, 160, 197-208.

Geosoft, 2000. Geosoft GridKnit, Grid stitching tool for OASIS montaj, Tutorial and user guide.

Götze, H.-J. and Lahmeyer, B., 1988. Application of three-dimensional interactive modeling in gravity and magnetics. *Geophysics*, 53(8): 1096-1108.

Kinck, J.J., Husebye, E.S. and Larsson, F.R., 1993. The Moho depth distribution in Fennoscandia and the regional tectonic evolution from Archean to Permian times, *Precambrian Research*, 64, 23-51.

Ludwig; J.W., Nafe, J.E. and Drake, C.L., 1970. Seismic refraction. In: Maxwell., A. (ed.): *The sea*, Vo.4, Wiley, New York.

Mauring, E., Mogaard, J.O. and Olesen, O., 2003. Røst Basin Aeromagnetic Survey 2003 (RAS-03). Ra 3 aeromagnetic compilation. Data acquisition and processing report. NGU Report 2003.070, 20pp.

- Mjelde, R., Sellevoll, M.A., Shimamura, H., Iwasaki, T. and Kanazawa, T., 1992. A crustal study off Lofoten, N. Norway, by use of 3D-component Ocean Bottom Seismographs. *Tectonophysics*, 212, 269-288.
- Mjelde, R., Kodaira, S., Shimamura, H., Kanazawa, T., Shiobara, H., Berg, E.W. and Riise, O., 1997. Crustal structure of the central part of the Vøring Basin, mid-Norway margin, from ocean bottom seismographs. *Tectonophysics*, 277, 235-257.
- Mjelde, R., Digranes, P., Shimamura, H., Shiobara, H., Kodaira, S., Brekke, H., Egjeberg, T., Sørenes, N. & Thorbjørnsen, S., 1998. Crustal structure of the northern part of the Vøring Basin, mid-Norway margin, from wide-angle seismic and gravity data. *Tectonophysics*, 293, 175-205.
- Mjelde, R., Digranes, P., van Schaack, M., Shimamura, H., Shiobara, H., Kodaira, S. & Naess O., 2001. Crustal structure of the outer Vøring Plateau, offshore Norway, from ocean bottom seismic and gravity data. *Journal of Geophysical Research*, 106, 6769-6791.
- Mjelde, R., Raum, T., Digranes, P., Shimamura, H., Shiobara, H. and Kodaira, S., 2003a.  $V_p/V_s$  ratio along the Vøring Margin, NE Atlantic, derived from OBS data: implications on lithology and stress field. *Tectonophysics*, 369, 175-197.
- Mjelde, R., Shimamura, H., Kanazawa, T., Kodaira, S., Raum T. and Shiobara, H., 2003b. Crustal lineaments, distribution of lower crustal intrusives and structural evolution of the Vøring Margin, NE Atlantic; new insight from wide-angle seismic models. *Tectonophysics* 369, 199-218.
- Mjelde, R., Iwasaki, T., Shimamura, H., Kanazawa, T., Kodaira, S., Raum, T. and Shiobara, H., 2003c. Spatial relationship between recent compressional structures and older high-velocity crustal structures; examples from the Vøring Margin, NE Atlantic, and Northern Honshu, Japan. *Journal of Geodynamics*, 36-4, 537-562.
- Norges geologiske undersøkelse, 1992. Aeromagnetisk anomalikart, Norge M 1:1 mill, Norges geologiske undersøkelse, Trondheim.
- Olesen, O. and Smethurst, M.A., 1995. NAS-94 interpretation Report, Part III: Combined interpretation of aeromagnetic and gravity data. NGU Report 95.040, 50 pp.
- Olesen, O., Torsvik, T.H., Tveten, E., Zwaan, K.B., Løseth, H. and Henningsen, T., 1997. Basement structure of the continental margin in the Lofoten-Lopphavet area, northern Norway: constraints from potential field data, on-land structural mapping and palaeomagnetic data. *Norsk Geologisk Tidsskrift*, 77, 15-33.

Olesen, O., Lundin, E., Nordgulen, Ø., Osmundsen, P.T., Skilbrei, J.R., Smethurst, M.A., Solli, A., Bugge, T. and Fichler, C., 2002. Bridging the gap between the onshore and offshore geology in Nordland, northern Norway. *Norwegian Journal of Geology*, 82, 243-262.

Osmundsen, P.T., Sommaruga, A., Skilbrei, J.R. and Olesen, O., 2002. Deep structure of the Mid Norway rifted margin. *Norwegian Journal of Geology*, 82, 205-224.

Planke, S., Skogseid, J. and Edholm, O., 1991. Crustal structure of Norway, 62° to 70° North. *Tectonophysics* 189, 91-107.

Raum, T., Mjelde, R., Digranes, P., Shimamura, H., Shiobara, H., Kodaira, S., Haatvedt, G., Sørensen, N. & Thorbjørnsen, T., 2002. Crustal structure of the southern part of the Vøring Basin, mid-Norway, from wide-angle seismic and gravity data. *Tectonophysics*, 355, 99-126.

Skilbrei, J.R., and Olesen, O., 2001. Structure of the basement in the Mid-Norwegian shelf interpreted from potential field data. In: E. Eide (ed.) BAT report: Status to December 2001, Geological Survey of Norway, Trondheim.

Skilbrei, J.R., Olesen, O., Osmundsen, P.T., Kihle, O., Aaro, S. and Fjellanger, E., 2002. A study of basement structures and onshore-offshore correlations in Central Norway. *Norwegian Journal of Geology*, 82, 263-279.

Schmidt, S. and Götze, H.-J., 1998. Interactive visualization and modification of 3D models using GIS functions. *Phys. Chem. Earth*, 23(3): 289-296.

Skogseid, J., Pedersen, T., Eldholm, O. and Larsen, B.T., 1992. Tectonism and magmatism during NE Atlantic continental break-up: the Vøring margin. In: B.C. Story, T. Alabaster and R.J. Plankhurst (Editors), *Magmatism and the Causes of Continental Break-up*. Geol. Soc. London, Spec. Publ., 68, 305-320.

Trinidad, N.D., 2003. Geophysical modeling of deep structures on the Mid-Norwegian continental shelf. Master thesis - Norges teknisk-naturvitenskapelige universitet (NTNU) Trondheim.

Wheeler, W., Karpuz, R., Mjelde, R., Torné, M. and van Schaack, M., 2002. Constraints on the geometry of the conjugate Norwegian and Greenland lower-crustal high-velocity body, or magmatic underplating. In: Jónsson, S.S. (Editor): 25th Nordic Geological Winter Meeting, Abstract Volume, 230.

Aarnæs, S., 2003. A geophysical study of deep geological structures of the Mid-Norwegian Continental Shelf. Master thesis - Norges teknisk-naturvitenskapelige universitet (NTNU) Trondheim.

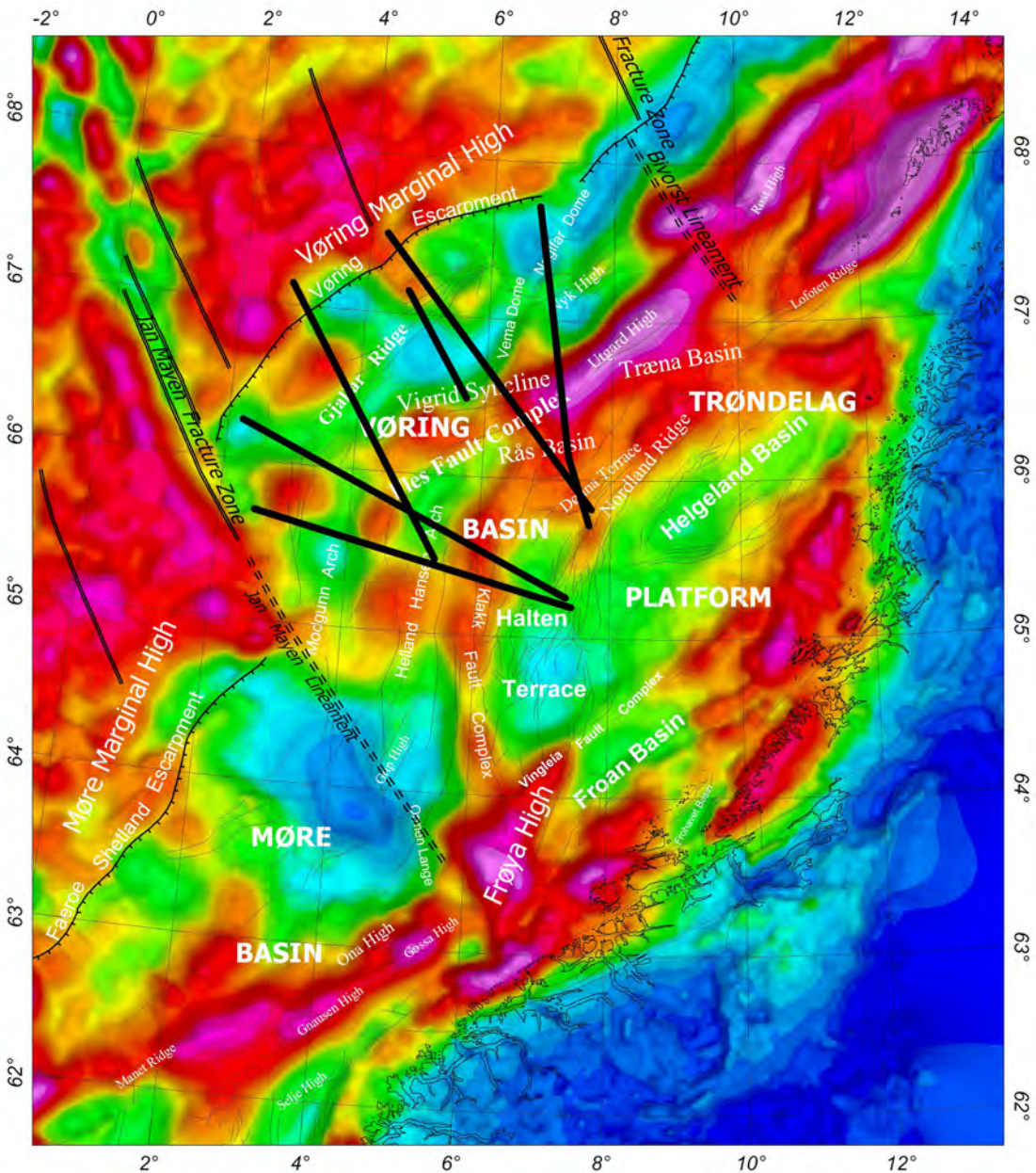


## LIST OF FIGURES AND TABLES

- Figure 1** Structural elements of the Mid-Norwegian Shelf
- Figure 2** Seismic profiles by BP and available OBS lines in the study area
- Figure 3** Location of gravity stations on the Norwegian continental shelf
- Figure 4** Gravity anomaly of the Norwegian continental shelf
- Figure 5** Offshore aeromagnetic surveys
- Figure 6** Magnetic field of the Norwegian continental shelf
- Figure 7** Bathymetry/topography of the Norwegian Shelf and the adjacent mainland
- Figure 8** Profile GVLO - 2D density structure, free-air- and magnetic anomaly
- Figure 9** Profile GVLO - Alternative interpretation
- Figure 10** Profile VMT - 2D density structure, free-air- and magnetic anomaly
- Figure 11** Profile VBT94 - 2D density structure and free-air anomaly
- Figure 12** The 3D model - Southern cross section
- Figure 13** The 3D model - Central cross section
- Figure 14** The 3D model - Northern cross section
- Figure 15** Profile GRS - 2D density structure, free-air- and magnetic anomaly
- Figure 16** Profile BPN - density structure, free-air- and magnetic anomaly
- Figure 17** Basement depth on the Mid-Norwegian Continental shelf
- Figure 18** Moho Depth on the Mid-Norwegian Continental Shelf
- Figure 19** Isostatic loads along the profiles GVLO and VBT94

- Table 1** Overview of the interpreted profiles by BP used in this study
- Table 2** Marine gravity surveys on the Mid-Norwegian continental shelf compiled for the present study
- Table 3** Offshore aeromagnetic surveys compiled for the present study
- Table 4** On land aeromagnetic surveys compiled for the present interpretation
- Table 5** Overview of reported densities of geological units on the Mid-Norwegian continental margin. Density values in  $\text{kg/m}^3$

- Map 1** Gravity anomaly of the Norwegian continental shelf
- Map 2** Magnetic field of the Norwegian continental shelf
- Map 3** Moho depth on the Mid-Norwegian Continental Shelf
- Map 4** Basement depth on the Mid-Norwegian Continental shelf

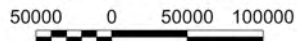


-80 -35 -15 -6 -2 2 4 6 8 9 11 15 18 22 25 29 34 39 47 59



mGal

Scale 1:1000000

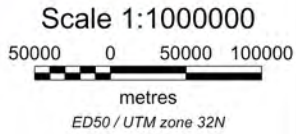
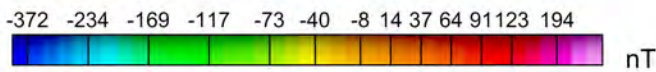
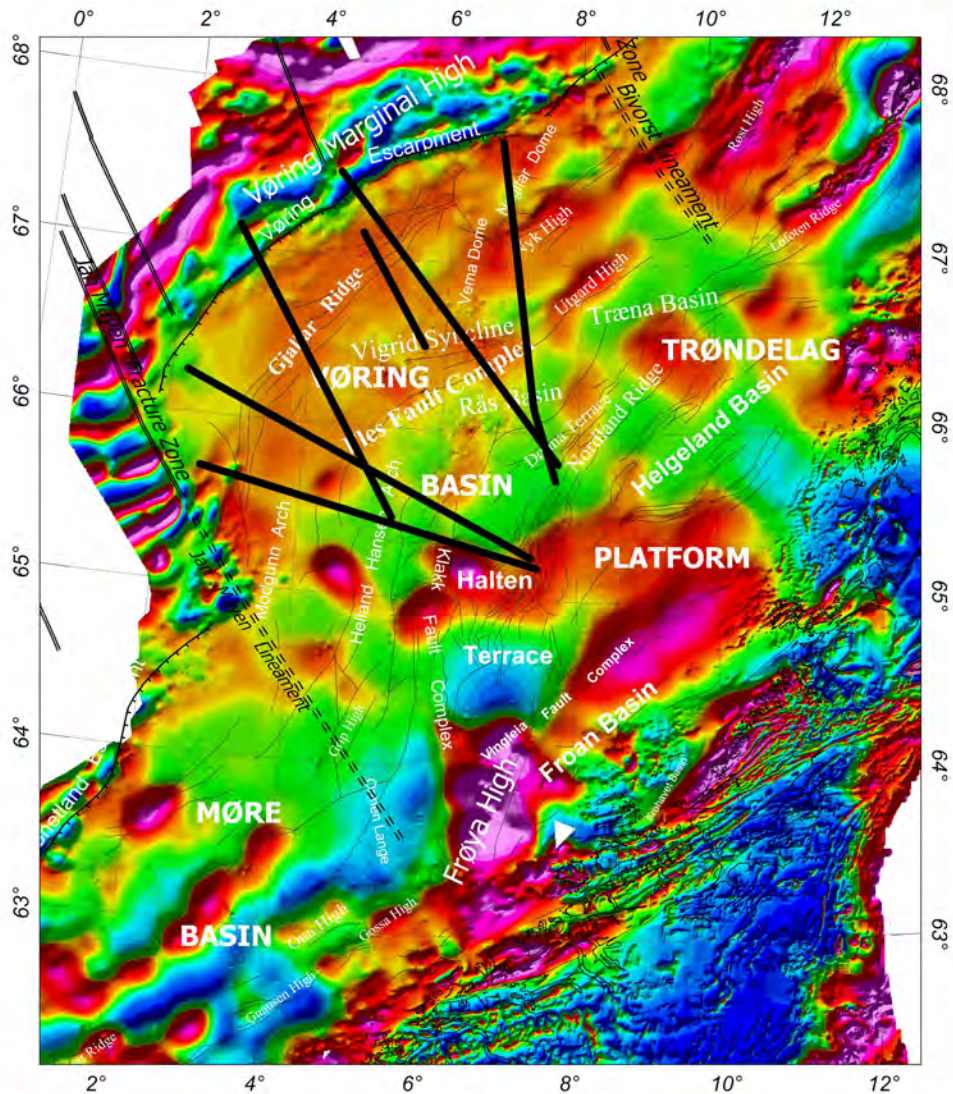


metres

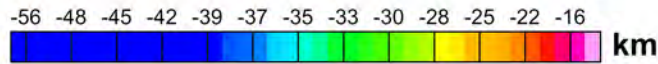
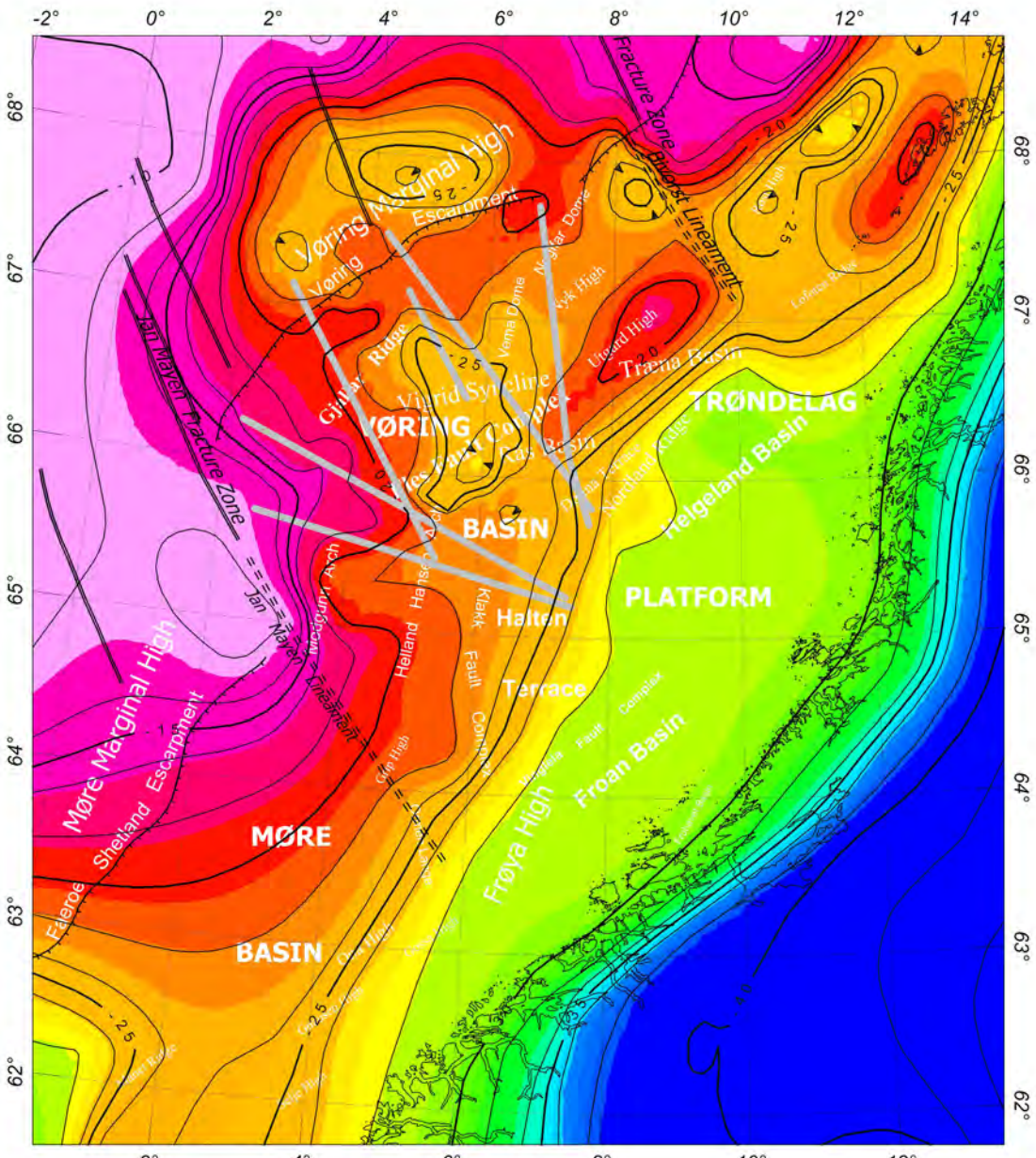
ED50 / UTM zone 32N



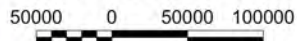
**Map 1: Gravity Anomaly Map**  
 Offshore: Free Air Anomaly, Onshore: Bouguer Anomaly



**Map 2: Magnetic Anomaly Map**



Scale 1:1000000



metres

ED50 / UTM zone 32N



**Map 3: Depth to Moho**

